

---

# Latent Q-Barrier Shielding for Safe In-Context Reinforcement Learning

---

**Minjae Kwon**<sup>\*†</sup>  
University of Virginia  
mjkwon@virginia.edu

**Amir Moeini**<sup>\*†</sup>  
University of Virginia  
amoeini@virginia.edu

**Shangdong Zhang**  
University of Virginia  
shangdong@virginia.edu

**Lu Feng**  
University of Virginia  
lu.feng@virginia.edu

## Abstract

Safe in-context reinforcement learning (ICRL) adapts online from interaction history without test-time parameter updates while controlling episode cost under a safety budget. Under out-of-distribution (OOD) deployment shifts, pretraining-only safe ICRL can give poor reward-safety tradeoffs because the remaining budget affects behavior only through frozen policy conditioning, not an explicit action-level check against predicted future cost. We propose a latent Q-Barrier shield that learns a context representation, latent dynamics, and an ensemble cost critic before deployment. Without parameter updates, the shield infers context from history and filters or softly reweights candidate actions using the remaining budget and predicted future cost. We prove a conditional, error-decomposed barrier-margin result: a Q-Barrier-satisfying action leaves the next latent-budget state with an approximately budget-safe continuation under the learned critic, up to Bellman and latent-prediction errors. Across five safe ICRL benchmarks, the shield improves deployment-time reward-safety tradeoffs over a strong safe-ICRL baseline: after a short context window, it achieves higher return in four of five benchmarks while matching or lowering average episode cost in all five.

## 1 Introduction

Reinforcement learning (RL) [55] agents deployed in the real world must manage safety constraints such as resource limits, physical damage, or constraint violations during deployment. Constrained Markov decision processes (CMDPs) [4] formalize this requirement by assigning each transition both a reward and a cost and constraining expected cumulative cost under a user-specified budget. Most safe RL methods enforce this constraint during training, for example through Lagrangian penalties or constrained policy optimization [1, 46].

In-context reinforcement learning (ICRL) provides a different adaptation mechanism: a pretrained agent adapts to new tasks at test time without parameter updates by conditioning its policy on an expanding interaction history [14, 63, 33, 53, 42, 36]. Recent work extends this idea to safe ICRL. In particular, Moeini et al. [40] formulate safe ICRL as a constrained problem across test episodes and propose SCARED, a Lagrangian pretraining method whose fixed-point analysis characterizes budget-respecting policies under its assumptions.

---

<sup>1\*</sup> Equal contribution.

<sup>2†</sup> Corresponding authors.

However, existing safe ICRL methods, such as SCARED, mainly encode safety through pretraining objectives or cost-conditioning, rather than through an explicit action-level check against the remaining budget. A frozen ICRL policy may still assign probability to actions whose predicted future cost exceeds the remaining budget, especially in generalization settings where the task and safety structure must be inferred from context. We add a budget-aware shielding layer that evaluates candidate actions against the remaining budget using a latent cost barrier and a pessimistic cost-to-go critic. The shield then filters or softly reweights the policy distribution without deployment-time parameter updates, turning learned safety preferences into an explicit action-level check.

This motivates the central question of the paper: *can a learned barrier improve a frozen safe-ICRL policy’s reward-safety tradeoff by turning the remaining budget into an explicit action-selection constraint?* We answer this question through a Q-Barrier shielding method, a margin-based analysis, and empirical evaluation on deployment generalization tasks. In summary, our contributions are:

- **Barrier-based runtime shielding for safe ICRL deployment.** We introduce a deployment-time shield that reweights a frozen policy using the remaining safety budget and a learned cost-to-go estimate. The shield uses latent representations, latent dynamics, and an ensemble cost critic learned during training, with all parameters fixed at deployment.
- **Budget-safe continuation analysis.** We prove a Q-Barrier margin bound showing that a shielded action preserves next-step latent-budget margin up to Bellman upper-bound and latent-prediction errors. A Q-Barrier-satisfying action thus admits an approximately budget-safe continuation under the learned critic.
- **Improved in-context adaptation reward-safety tradeoffs.** Q-Barrier improves early return and lowers cost after a short context window in four of five benchmarks, with one environment showing a conservative lower-cost/lower-return tradeoff. In budget sweeps, it achieves the highest cumulative return in four of five environments and satisfies the budget across most levels, with violations mostly occurring at near-zero budgets, where even small costs can exceed the budget.

## 2 Background

**Markov Decision Processes.** We model the interaction with an environment as a finite-horizon Markov decision process (MDP [44]). An MDP is defined by a state space  $\mathcal{S}$ , an action space  $\mathcal{A}$ , a reward function  $r : \mathcal{S} \times \mathcal{A} \rightarrow \mathbb{R}$ , a transition kernel  $p(\cdot | s, a)$ , where for each state-action pair  $(s, a)$ ,  $p(\cdot | s, a)$  denotes a probability distribution over next states in  $\mathcal{S}$ , an initial state distribution  $p_0$  over  $\mathcal{S}$ , and a horizon length  $T$ . We denote by  $T_k$  the terminal timestep of episode  $k$ . An agent follows a stochastic policy  $\pi$ , modeled as a Markov kernel from states to actions: for each  $s \in \mathcal{S}$ ,  $\pi(\cdot | s)$  is a probability distribution over  $\mathcal{A}$ . When  $\mathcal{A}$  is discrete,  $\pi(a | s)$  denotes the probability mass of action  $a$ . When  $\mathcal{A}$  is continuous,  $\pi(a | s)$  denotes the action density, when it exists, which integrates to one. After starting from  $S_0 \sim p_0$ , at time step  $t$ , the agent samples  $A_t \sim \pi(\cdot | S_t)$ , observes reward  $R_{t+1} \doteq r(S_t, A_t)$ , and transitions to  $S_{t+1} \sim p(\cdot | S_t, A_t)$ . We use  $k$  to index episodes and  $t$  to index time steps within an episode. For any episode  $\tau$ , we define its return as  $G(\tau) \doteq \sum_{t=1}^T R_t$ . The performance of a policy  $\pi$  is measured by the expected total rewards  $J(\pi) \doteq \mathbb{E}_{\tau \sim \pi}[G(\tau)]$ .

**Constrained Markov Decision Processes.** In addition to the reward function  $r$ , a constrained MDP (CMDP [4]) involves a cost function  $c : \mathcal{S} \times \mathcal{A} \rightarrow \mathbb{R}^+$  with an associated user-given budget  $\delta$ . At each time step  $t$ , after taking an action  $A_t$  at a state  $S_t$ , the agent receives a cost  $C_{t+1} \doteq c(S_t, A_t)$ . An episode in a CMDP therefore becomes  $\tau = (S_0, A_0, R_1, C_1, S_1, \dots, S_{T-1}, A_{T-1}, R_T, C_T)$ . We denote the total cost of an episode  $\tau$  by  $G_c(\tau) \doteq \sum_{t=1}^T C_t$ , which should, in expectation, remain below the budget  $\delta$ . The return-to-go (RTG) is  $G_t(\tau) \doteq \sum_{i=t+1}^T R_i$  and the cost-to-go (CTG) is  $G_{c,t}(\tau) \doteq \sum_{i=t+1}^T C_i$ . Given  $\delta$ , we define the remaining cost budget at time  $t$  as  $B_t \doteq \delta - \sum_{i=1}^t C_i$ ,  $B_0 = \delta$ .

**In-Context Reinforcement Learning.** ICRL [39] trains an agent across a distribution of tasks so that, at test time, it can adapt without parameter updates by conditioning on an expanding interaction history. Let  $\theta_*$  denote the pretrained parameters. During deployment,  $\theta_*$  is fixed and the policy is written as  $\pi_{\theta_*}(\cdot | S_t^k, H_t^k)$ , where  $H_t^k$  is the context available at time  $t$  in episode  $k$ . A context consists of previous episodes  $\{\tau_j\}_{j=1, \dots, k-1}$  and the current episode prefix  $\tau_k^t$ , i.e.,  $H_t^k \doteq (\tau_1, \dots, \tau_{k-1}, \tau_k^t)$ . In safe ICRL [40], each task is a CMDP, so the context includes both rewards and costs:  $\tau_k^t \doteq (S_0^k, A_0^k, R_1^k, C_1^k, S_1^k, \dots, S_{t-1}^k, A_{t-1}^k, R_t^k, C_t^k)$ . We write the remaining

episode budget as  $B_t^k \doteq \delta - \sum_{i=1}^t C_i^k$ ,  $B_0^k = \delta$ . Adaptation occurs as  $\pi_{\theta_*}(\cdot | S_t^k, H_t^k)$  changes with the growing context, while the policy parameters remain fixed.

## 2.1 Problem Formulation

We formulate safe ICRL deployment over  $K$  test episodes. All parameters are learned before deployment and fixed at test time. The deployed shielded policy  $\pi$  uses the current state  $S_t^k$ , context  $H_t^k$ , and remaining budget  $B_t^k$  for action selection. Our objective is:

$$\max_{\pi} \sum_{k=1}^K \mathbb{E}_{\pi}[G(\tau_k)] \quad \text{s.t.} \quad \frac{1}{K} \sum_{k=1}^K \mathbb{E}_{\pi}[G_c(\tau_k)] \leq \delta. \quad (1)$$

The shield changes actions online to improve reward-safety tradeoffs during deployment. Theorem 1 shows how the barrier margin propagates one step forward and when the next state still admits an approximately budget-safe continuation under the learned critic. Proposition 1 shows an episode-level budget-bound.

## 3 Approach

We present the method in three parts. First, we define the latent state and learned safety model used for runtime safety estimation. Second, we introduce a Q-function barrier that uses the learned cost-to-go estimate and the remaining safety budget to filter actions online. Third, we describe how the latent representation, dynamics model, and cost critic are trained to support shielding at deployment.

### 3.1 Latent State and Projection Spaces

The shield uses two views of the same in-context state: a policy view for proposing actions and a world view for evaluating safety. Let  $\mathcal{H}$  denote the context space and let  $E_{\phi} : \mathcal{H} \times \mathcal{S} \rightarrow \mathcal{Z} \subseteq \mathbb{R}^{d_z}$  be the shared encoder. Given context  $H_t^k$  and state  $S_t^k$ , the shared latent state is  $Z_t^k \doteq E_{\phi}(H_t^k, S_t^k) \in \mathcal{Z}$ . From this shared latent, we define two projection heads with a common projected dimension  $d_m$ :  $g_{\omega}^{\text{world}} : \mathcal{Z} \rightarrow \mathcal{Z}^w \subseteq \mathbb{R}^{d_m}$ ,  $g_{\psi}^{\text{policy}} : \mathcal{Z} \rightarrow \mathcal{Z}^p \subseteq \mathbb{R}^{d_m}$ . The corresponding projected latents are  $Z_t^{w,k} \doteq g_{\omega}^{\text{world}}(Z_t^k)$ ,  $Z_t^{p,k} \doteq g_{\psi}^{\text{policy}}(Z_t^k)$ . The world-projected latent  $Z_t^{w,k}$  is the safety and modeling space used by the latent dynamics model, cost critic, and runtime barrier. The policy-projected latent  $Z_t^{p,k}$  is the policy-side representation used by the base policy to form its action distribution. The shield proposes actions through the policy view and evaluates their budget risk through the world view. On  $\mathcal{Z}^w$ , we learn a probabilistic latent transition model  $p_z(\cdot | Z_t^{w,k}, A_t^k)$  and an ensemble of cost critics  $\{\hat{Q}_{C,i}\}_{i=1}^M$ . The deployed shield uses the pessimistic aggregate  $\hat{Q}_C^+(Z, A) \doteq \max_{i \in \{1, \dots, M\}} \hat{Q}_{C,i}(Z, A)$ , which reduces the risk of underestimating future cost. We write  $f_z(Z_t^{w,k}, A_t^k) \doteq \mathbb{E}_{p_z}[Z_{t+1}^{w,k} | Z_t^{w,k}, A_t^k]$  for the predictive mean. The critic  $\hat{Q}_C^+$  estimates conservative cumulative cost-to-go, while  $f_z$  is the deterministic prediction used in the barrier construction and theoretical analysis. All modules are learned during training and frozen at test time.

### 3.2 Q-Function Barrier and Shield Policy

The shield maps a base policy into a budget-aware action distribution. During training, the base policy  $\pi_{\theta}$  is updated. At each decision time  $t$  in episode  $k$ , the shield evaluates a finite candidate action set  $\mathcal{A}_{t,k}^{\text{cand}} \subseteq \mathcal{A}$ . In discrete-action settings,  $\mathcal{A}_{t,k}^{\text{cand}} = \mathcal{A}$ ; in continuous-action settings, it is the finite set of candidate actions sampled from  $\pi_{\theta}$ . At state  $Z_t^{w,k}$  with remaining budget  $B_t^k$ , actions whose predicted cost-to-go exceeds the available budget are discouraged. This motivates a learned barrier signal derived from the cost critic: the value is positive when the remaining budget suffices to cover the predicted cost-to-go and negative when the action is predicted to overspend the budget. Because the barrier depends on the current latent state and learned cost-to-go estimate, it adapts online as context accumulates, without changing any parameters.

**Definition 1 (Q-Function Barrier).** For  $Z \in \mathcal{Z}^w$ , define the candidate-set cost value  $\hat{V}_{C,t}^{+,k}(Z) \doteq \min_{A \in \mathcal{A}_{t,k}^{\text{cand}}} \hat{Q}_C^+(Z, A)$ . The state- and state-action barriers are

$$b_{V,t}^k(Z_t^{w,k}, B_t^k) \doteq B_t^k - \hat{V}_{C,t}^{+,k}(Z_t^{w,k}), \quad b_{Q,t}^k(Z_t^{w,k}, B_t^k, A_t^k) \doteq B_t^k - \hat{Q}_C^+(Z_t^{w,k}, A_t^k). \quad (2)$$

The state barrier  $b_{V,t}^k \geq 0$  means that at least one candidate action has predicted cost-to-go no larger than the remaining budget. The action barrier  $b_{Q,t}^k$  evaluates whether a specific action is predicted to stay within the remaining budget under  $\hat{Q}_C^+$ . Because this margin is estimated by learned models, we use it as a soft risk signal rather than a hard certificate. The primary variant is a *soft shield* that reweights  $\pi_\theta$  over  $\mathcal{A}_{t,k}^{\text{cand}}$ , preserving policy support while penalizing candidates whose predicted cost exceeds the remaining budget. For notational convention, we use  $[x]_+ \doteq \max\{x, 0\}$ . For each candidate action, define the soft-shield score as

$$w_t(A) \doteq \rho_t(A) \exp\left(-\left[-b_{Q,t}^k(Z_t^{w,k}, B_t^k, A)\right]_+\right), \text{ where}$$

$$\rho_t(A) = \begin{cases} \pi_\theta(A | Z_t^{p,k}), & \text{if the discrete action space is enumerated,} \\ 1, & \text{if } A \in \mathcal{A}_{t,k}^{\text{cand}} \text{ is sampled from } \pi_\theta(\cdot | Z_t^{p,k}). \end{cases}$$

Then, the soft-shield distribution over the finite candidate set is

$$\pi_{\text{soft}}(A | S_t^k, H_t^k, B_t^k) = \frac{w_t(A)}{\sum_{A' \in \mathcal{A}_{t,k}^{\text{cand}}} w_t(A')}, \quad A \in \mathcal{A}_{t,k}^{\text{cand}}. \quad (3)$$

**Remark.** We use the soft shield as the default because it preserves support over sampled candidates and avoids sensitive hard-threshold decisions. Hard filtering can be sensitive to model or critic error: when no candidate is considered as feasible, it falls back to the lowest-predicted-cost action. Empirically, both variants achieve similar reward–safety profiles in most environments (Appendix D). Unlike hard filtering in Appendix C, it can still choose an action with  $b_{Q,t}^k < 0$ . In continuous control, candidates are already drawn from the base policy, so we omit an additional policy-density factor in the finite-candidate weights to avoid double-counting the proposal.

### 3.3 Training Objective and Asymmetric Gradient Routing

The shield uses  $Z_t^{p,k}$  for action proposals and  $Z_t^{w,k}$  for latent prediction and cost estimation. All modules are trained before deployment and then frozen. To reduce interference between policy learning and world modeling, we use asymmetric gradient routing: the world-model loss updates the shared encoder, while stop-gradient alignment losses coordinate the projection heads without directly updating the encoder.

**Representation-shaping loss.** We train an auxiliary one-step world model on the world-projected latent space. The loss is  $\mathcal{L}_{\text{wm}} = \mathbb{E}[-\log p_z(Z_{t+1}^{w,k} | Z_t^{w,k}, A_t^k)] + \mathbb{E}[(\hat{R}_{t+1}^k - R_{t+1}^k)^2] + \mathbb{E}[(\hat{C}_{t+1}^k - C_{t+1}^k)^2]$ . This loss trains the encoder and world projection by encouraging one-step predictability of latent dynamics, reward, and cost.

**Structural alignment losses.** The losses  $\mathcal{L}_{\text{distill}}$  and  $\mathcal{L}_{\text{conj}}$  align the policy and world projections through detached encoder features:  $\mathcal{L}_{\text{distill}}^{\text{sg}} = \left\| g_\psi^{\text{policy}}(\text{sg}(Z_t^k)) - \text{sg}(g_\omega^{\text{world}}(Z_t^k)) \right\|_2^2$ , and

$$\mathcal{L}_{\text{conj}}^{\text{sg}} = \left\| (g_\psi^{\text{policy}}(\text{sg}(Z_{t+1}^k)) - g_\psi^{\text{policy}}(\text{sg}(Z_t^k))) - \text{sg}(g_\omega^{\text{world}}(Z_{t+1}^k) - g_\omega^{\text{world}}(Z_t^k)) \right\|_2^2.$$

Combining the actor, critic, and auxiliary losses gives the full training objective

$$\mathcal{L}_{\text{total}} = \mathcal{L}_{\text{actor}} + \lambda_{\text{critic}} \mathcal{L}_{\text{critic}} + \lambda_{\text{wm}} \mathcal{L}_{\text{wm}} + \lambda_{\text{dist}} \mathcal{L}_{\text{distill}}^{\text{sg}} + \lambda_{\text{conj}} \mathcal{L}_{\text{conj}}^{\text{sg}}, \quad (4)$$

where  $\text{sg}$  denotes stop-gradient with respect to the encoder. Asymmetric gradient routing encourages  $Z^w$  to support latent prediction and cost estimation while preserving policy-relevant features in  $Z^p$ .

## 4 Barrier Margin Propagation

This section gives a decomposition of the next-step barrier value into three quantities: the current barrier margin, the one-step latent prediction error, and the Bellman upper-bound error of the learned cost critic. For any fixed next-step candidate set  $\mathcal{A}_{t+1,k}^{\text{cand}}$ , define  $\hat{V}_{C,t+1}^{+,k}(Z) \doteq \min_{A' \in \mathcal{A}_{t+1,k}^{\text{cand}}} \hat{Q}_C^+(Z, A')$ ,

with  $\hat{V}_{C,T_k}^{+,k} = 0$ . In continuous-action domains,  $\mathcal{A}_{t+1,k}^{\text{cand}}$  is the finite set of candidate actions sampled by the shield, so all statements are conditional on the sampled candidate set.

We first assume that the learned latent dynamics model predicts the next latent state with small one-step error, motivated by the training objective in Section 3.3.

**Assumption 1** (Approximate Latent Dynamics). *Along the trajectories considered, the learned latent transition mean  $f_z$  satisfies  $\|f_z(Z_t^{w,k}, A_t^k) - Z_{t+1}^{w,k}\|_2 \leq \varepsilon_{\text{pred}}$  for all episodes  $k$  and timesteps  $t$ .*

We also assume that the learned cost critic changes smoothly when the latent state changes slightly.

**Assumption 2** (Latent Q-Regularity). *For  $A$  in the candidate action set, the pessimistic cost critic  $\hat{Q}_C^+ : \mathcal{Z}^w \times \mathcal{A} \rightarrow \mathbb{R}$  is uniformly Lipschitz. That is, there exists  $L_Q > 0$  such that*

$$\left| \hat{Q}_C^+(Z, A) - \hat{Q}_C^+(Z', A) \right| \leq L_Q \|Z - Z'\|_2 \quad \text{for all } Z, Z' \in \mathcal{Z}^w. \quad (5)$$

We next isolate the critic’s one-step Bellman error as an explicit residual term.

**Definition 2** (Bellman Upper-Bound Error). *For transition  $(Z_t^{w,k}, A_t^k, C_{t+1}^k)$ , define*

$$\Delta_{\text{bell},t}^{+,k} \doteq \left[ C_{t+1}^k + \hat{V}_{C,t+1}^{+,k} \left( f_z(Z_t^{w,k}, A_t^k) \right) - \hat{Q}_C^+(Z_t^{w,k}, A_t^k) \right]_+. \quad (6)$$

This value measures how much the critic violates the one-step Bellman upper bound.  $\Delta_{\text{bell},t}^{+,k} = 0$  when the critic holds the one-step upper-bound condition  $\hat{Q}_C^+(Z_t^{w,k}, A_t^k) \geq C_{t+1}^k + \hat{V}_{C,t+1}^{+,k} (f_z(Z_t^{w,k}, A_t^k))$ . The main theorem below shows how the barrier margin propagates forward by losing Bellman error and model-prediction error.

**Theorem 1** (Barrier Margin Propagation on the Latent Space). *Under Assumptions 1 and 2, for any selected action  $A_t^k$ ,  $b_{V,t+1}^k(Z_{t+1}^{w,k}, B_{t+1}^k) \geq b_{Q,t}^k(Z_t^{w,k}, B_t^k, A_t^k) - \Delta_{\text{bell},t}^{+,k} - L_Q \varepsilon_{\text{pred}}$ .*

The theorem implies an approximate one-step continuation property: if  $b_{Q,t}^k(Z_t^{w,k}, B_t^k, A_t^k) \geq 0$ , then  $b_{V,t+1}^k(Z_{t+1}^{w,k}, B_{t+1}^k) \geq -\Delta_{\text{bell},t}^{+,k} - L_Q \varepsilon_{\text{pred}}$ . Thus, the next latent-budget state remains approximately feasible up to Bellman and prediction errors. With enough positive barrier margin, it has a nonnegative continuation margin. This is a conditional statement about the selected action, not a closed-loop guarantee for the soft shield, which may still sample actions with  $b_{Q,t}^k < 0$ . For continuous-action settings, action selections are over the finite candidate set evaluated by the shield. See Appendix A for proofs, and Appendix A.2 for an episode-level budget bound.

## 5 Experiments

We evaluate our method on the safe ICRL benchmark [40], comparing against safe ICRL methods [40] and safe meta-RL baselines augmented with a context encoder [15, 64]. Our experiments are designed to answer two questions: (i) whether shielding improves the reward-safety tradeoff during in-context adaptation without parameter updates, and (ii) how this tradeoff changes as the safety budget varies.

### 5.1 Baselines

We compare against two baseline groups. The first consists of parameter-update-free safe adaptation methods, which adapt through context at test time without gradient updates. This group includes Safe AD and SCARED, which differ mainly in how safety is learned during pretraining. The second consists of safe meta-RL methods, which adapt through per-task parameter updates at test time.

**Safe Algorithm Distillation (Safe AD).** Following algorithm distillation [33], Safe AD [40] trains a history-conditioned policy on logged learning trajectories generated by safe RL algorithms. At test time, the policy conditions on the interaction history together with RTG and CTG targets, without any parameter updates.

**SCARED.** This is the state-of-the-art safe ICRL baseline trained with an exact-penalty dual objective to improve reward-safety tradeoffs through in-context adaptation [40]. We use SCARED as the base policy for our shield.

**Safe Meta-RL.** We compare against gradient-based safe meta-RL methods: MAML with penalty [15] and SafeMeta [64]. MAML with penalty learns a cost-regularized initialization, while SafeMeta meta-trains a closed-form one-step safe adaptation rule. Unlike in-context baselines, both adapt through parameter updates rather than conditioning on cross-episode histories.

## 5.2 Experimental Setup

**Safe ICRL Benchmarks.** We evaluate our approach on three safe ICRL benchmarks [40] studying two complementary generalization regimes: *structural OOD* tasks and *unseen ID* tasks. For structural OOD generalization, we use SafeDarkRoom and SafeDarkMujoco (Point, Car), where test tasks involve shifted goal and obstacle configurations under partial observability: Range-based sensing (e.g., lidar) is unavailable, so the agent cannot directly observe goal or obstacle locations and must adapt from in-context history. For unseen ID generalization, we use SafeVelocity (HalfCheetah, Ant), where each task is specified by a target velocity. We train on a subset of target velocities from a fixed range and evaluate on held-out velocities from the same range. See Appendix G for more details.

**Training Setup.** For the structural OOD environments, all algorithms are trained on source tasks with center-oriented obstacles and goals and evaluated on 100 OOD test tasks with edge-oriented obstacle and goal distributions. For the unseen-ID environments, target-velocity multipliers are sampled uniformly from [0.5, 2.0] during training. We evaluate each method on 100 held-out contexts sampled from the same range, keeping the target velocity fixed across the in-context episode adaptation.

Safe AD follows the training protocol of [40], using trajectories generated by PPO-Lag [46] and the training hyperparameters. We use SCARED as the base policy and keep its original pretraining budgets: 3K epochs for SafeDarkRoom and SafeDarkMujoco, and 2K for SafeVelocity. An epoch is one collection-update cycle, consisting of 1.5K environment steps per training environment followed by 1K optimization batches. The shield-supporting modules in Section 3 are trained during this same pretraining phase, with no additional epochs. At test time, Q-Barrier shield reweights candidate actions using Equation (3), without parameter updates. Safe meta-RL baselines are trained for up to 15K meta-training steps on each environment, with most converging earlier. For Safe AD and the safe meta-RL baselines, we perform hyperparameter optimization to ensure a fair comparison. All loss weights in Equation (4) for our shield-supporting modules are fixed across environments. See Appendix H for full hyperparameters and compute details.

**Evaluation Setup.** To answer the two research questions, we use a consistent target-conditioning setup across methods. For SCARED and our Q-Barrier, we evaluate robustness to safety budgets by conditioning on CTG values sampled uniformly from [1, 15] in SafeDarkRoom, [10, 50] in SafeDarkMujoco, and [0, 5] in SafeVelocity, and we report performance averaged over 100 distinct CTG targets. Q-Barrier uses the soft shield with a candidate-set size of  $N_s = 8$  in continuous-action environments. The same CTG intervals and number of targets are used for SafeMeta, MAML with penalty, and Safe AD. For Safe AD, following [40], we use paired RTG-CTG conditioning: each CTG target sampled from the same interval is paired with a corresponding RTG target. In SafeDarkRoom and SafeDarkMujoco, RTG is set as  $\max\{0.1, \text{CTG}/\text{CTG}_{\max}\}$  with  $\text{CTG}_{\max} = 15$  and 50, respectively. In the unseen-ID tasks, RTG and CTG are jointly scaled from 0.5 to  $\text{RTG}_{\max} = 200$ , and  $\text{CTG}_{\max} = 5$  for both. Values report means over the 100 evaluation rollouts in Figures 1 and 2, with shaded regions denoting standard error of the mean.

## 5.3 Results Analysis

### RQ1: Does shielding improve the reward-safety tradeoff during in-context adaptation without parameter updates?

We compare Q-Barrier and the baselines over in-context episodes on OOD test tasks, measuring how return and cost evolve as context accumulates (Figure 1). Since Q-Barrier uses SCARED as its base policy, the most direct comparison is against SCARED. Safe AD, Safe Meta, and MAML with penalty provide additional safe ICRL and safe meta-RL baselines. During OOD adaptation, these baselines fail to reduce cost consistently or become overly conservative sacrificing return.

Q-Barrier generally improves the in-context adaptation by reaching high return earlier while reducing cost after a short context window. In SafeDarkRoom and SafetyAnt, the improvement is immediate. In SafeDarkRoom, Q-Barrier achieves mean return 0.9 compared with 0.62 for SCARED, a 46%

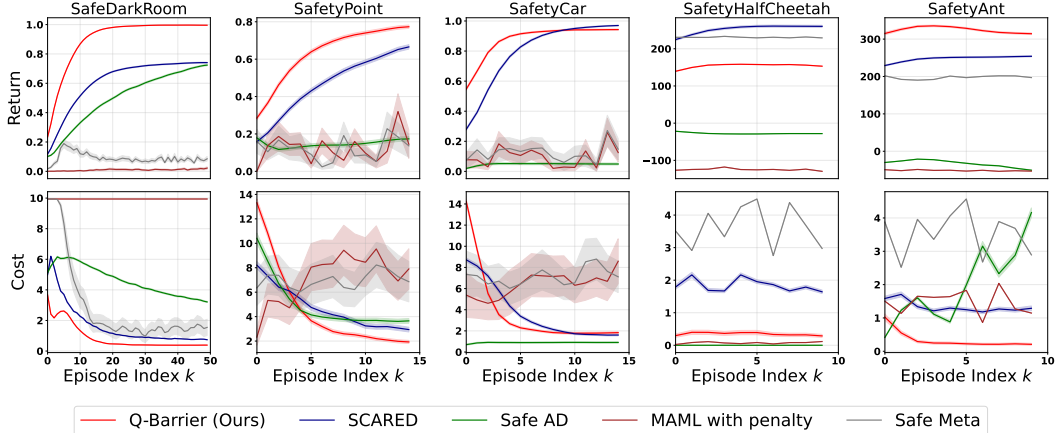


Figure 1: **In-context adaptation dynamics (RQ1)**. Per-episode return (top) and cost (bottom) over in-context episode index  $k$  on test-time evaluation tasks. Curves show means over 100 evaluation tasks, with shaded regions denoting standard error of the mean. Q-Barrier generally improves adaptation by reaching high return earlier and reducing cost after a short context window, while SafetyHalfCheetah shows a conservative Pareto point with lower cost and lower return.

gain, while reducing mean cost from 1.66 to 0.87, a 47.2% drop. In SafetyAnt, Q-Barrier achieves mean return 324.36 compared with 247.8 for SCARED, a 30.9% gain, while reducing mean cost from 1.34 to 0.34, a 74.3% drop.

DarkMujoco navigation tasks show a different but informative pattern: Q-Barrier initially encounters higher cost, but this early cost comes with higher return. In SafetyPoint and SafetyCar, Q-Barrier first becomes lower-cost than SCARED at episodes  $k = 3$  and  $k = 2$ , respectively. Averaged over the remaining adaptation, Q-Barrier reduces mean cost from 4.0 to 2.99 in SafetyPoint, a 25.3% drop, and from 2.95 to 2.37 in SafetyCar, a 19.7% drop. At the same time, Q-Barrier maintains an early return advantage in both tasks. For example, in SafetyCar, Q-Barrier exceeds return 0.9 by episode  $k = 5$ , whereas SCARED reaches this level around episode  $k = 7$ .

SafetyHalfCheetah is the main conservative case. During the full in-context adaptation, Q-Barrier consistently lowers cost but also lowers return relative to SCARED. Averaged over the adaptation, it reduces mean cost from 1.84 to 0.35, a 81.0% drop, while mean return decreases from 252.75 to 154.26, a 39.0% drop. This places Q-Barrier at a more conservative point on the reward-cost frontier. The results in Appendix B provide a plausible explanation: SafetyHalfCheetah has the largest latent prediction error among the evaluated environments, which can make the learned barrier more conservative.

*Takeaway: Q-Barrier improves the OOD reward-safety tradeoff during in-context adaptation, with SafetyHalfCheetah showing a conservative Pareto point that trades lower return for lower cost.*

## RQ2: How does the reward-safety tradeoff change across safety budgets?

We next evaluate the objective in Equation (1) by sweeping the cost budget and measuring cumulative return together with average episode cost over the in-context adaptation.

Figure 2 shows that Q-Barrier achieves the highest cumulative return in four of five environments across different budgets: SafeDarkRoom, SafetyPoint, SafetyCar, and SafetyAnt. It also satisfies the average episode-cost constraint across most budget settings in the sweep. Violations occur only at near-zero budgets, where even small residual costs exceed the requested budget. This is the most difficult setting for Q-Barrier, since small model or critic errors can produce a violation when the allowed cost is near zero.

Compared with SCARED base policy, Q-Barrier improves average cumulative return over budget levels by 54.4% in SafeDarkRoom, 36.3% in SafetyPoint, 10.1% in SafetyCar, and 31.0% in SafetyAnt. These gains are not obtained by simply spending more cost. Q-Barrier also reduces average episode cost relative to SCARED by 44.1% in SafeDarkRoom, 2.1% in SafetyPoint, 1.0% in SafetyCar, and

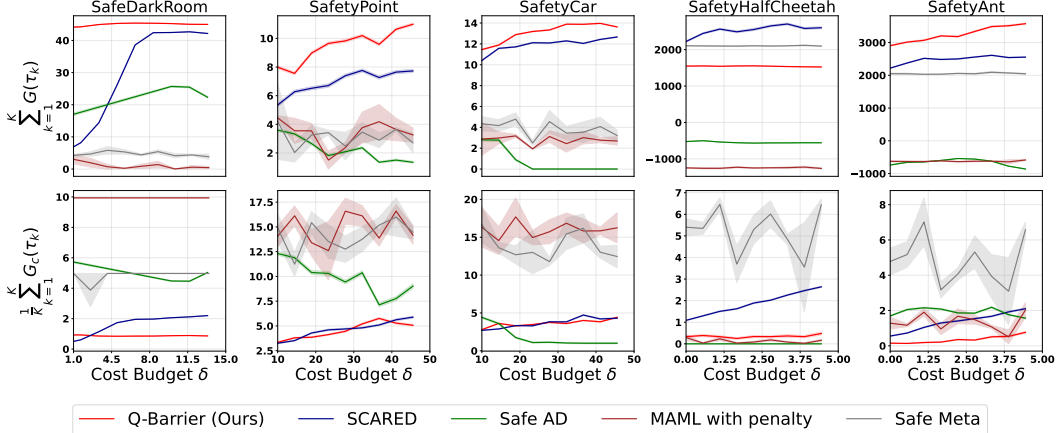


Figure 2: **Reward-cost tradeoffs under budget variation (RQ2)**. Cumulative reward (top) and average episode cost (bottom) over varying cost budgets on test-time evaluation tasks. Across different budget levels, Q-Barrier achieves the highest cumulative return in four of five environments while maintaining budget compliance in most cases, with violations mostly limited to near-zero budgets. Shaded regions denote standard errors of the mean over 100 evaluation tasks.

74.2% in SafetyAnt. Thus, in most environments, Q-Barrier improves return without increasing average cost, and in SafeDarkRoom and SafetyAnt it improves both return and cost by large margins.

SafeDarkRoom demonstrates the benefit of explicit budget-aware action selection. SCARED becomes conservative as the budget varies and does not fully convert available budget into return. In particular, given budget near 1, Q-Barrier exceeds return 40 while satisfying budget constraints, but SCARED stays under return 10.

SafetyHalfCheetah is the main exception. Q-Barrier reduces average episode cost by 81.3% relative to SCARED, but its cumulative return is 39.1% lower. Safe Meta also achieves higher cumulative return than Q-Barrier, but Safe Meta often violates the cost budget by a large margin (e.g., average cost around 6 when cost budget is 1). This is consistent with the conservative behavior observed in RQ1, which can be explained by the largest latent prediction error.

*Takeaway: Q-Barrier improves the OOD reward-safety frontier across budget levels in most environments, often increasing return while matching or reducing cost. SafetyHalfCheetah remains the conservative case, trading lower return for substantially lower cost.*

**Ablation Studies.** We include ablations and diagnostics for the main shielding design choices. First, we compare the soft shield (Equation 3) against a hard truncation variant that restricts candidates to those with nonnegative barrier margin, formally defined in Appendix C. The soft shield matches the hard shield’s reward-safety tradeoffs while preserving broader action support during early adaptation. Since hard filtering provides marginal and non-uniform cost reductions, we use soft reweighting in all main experiments (Appendix D). Second, we study how the number of sampled candidate actions  $N_s$  affects shielding in continuous-control environments, sweeping  $N_s \in \{4, 8, 16, 32\}$ . Performance is stable across  $N_s$  in SafeDarkMujoco, while SafeVelocity is more affected by  $N_s$ : larger candidate sets raise both return and cost (Appendix E). Appendix B reports empirical measurements of the learned quantities appearing in the barrier-margin bound (Theorem 1), including latent prediction error, critic sensitivity, and Bellman residuals, confirming that larger errors correlate with the conservative shielding observed in SafetyHalfCheetah. Appendix F provides pseudocode for the training and runtime shielding procedures, Appendix G describes the benchmark environments and OOD generation protocol, and Appendix H lists full hyperparameters for all methods.

## 6 Related Work

**Safe Reinforcement Learning.** Safe reinforcement learning is commonly formalized through constrained Markov decision processes (CMDPs), where policies maximize reward subject to expected cost constraints. Existing methods include constrained policy optimization, Lagrangian and primal-

dual algorithms, projection-based policy optimization, recovery policies, model-based safe RL, and sample-efficient constraint-handling methods [1, 57, 46, 69, 67, 66, 20, 5]. Runtime shielding provides a complementary mechanism by filtering, modifying, or replacing actions before execution [3, 7, 68], and recent safe planning and shielding methods use adaptive conformal prediction to calibrate uncertainty in safety-critical decision making [35, 51, 52, 47]. Control barrier functions provide certificate-based safety guarantees, but constructing valid barriers under learned, uncertain, or varying dynamics often requires explicit model knowledge or robust uncertainty bounds [11, 10, 16, 61, 62]. Our work is complementary to these methods: we introduce a budget-aware Q-Barrier shield for frozen in-context RL policies.

**In-Context Reinforcement Learning and Safe Adaptation.** In-context reinforcement learning (ICRL) studies agents that adapt to new tasks at test time without updating parameters, by conditioning the policy on an expanding interaction history [39]. This perspective is closely related to meta-RL, and contextual or hidden-parameter RL, where agents infer task or dynamics information from history and use it to improve behavior online [15, 65, 8, 9, 6]. Recent ICRL methods use transformers, recurrent models, state-space models, or algorithm-distillation objectives to induce adaptation behavior in the forward pass of a pretrained policy [14, 58, 63, 34, 33, 45, 28, 12, 13, 30, 17, 18, 59, 60]. Safe meta-RL extends fast adaptation to constrained settings, but often relies on explicit task-level adaptation, gradient updates, or additional offline adaptation data [38, 26, 21, 64]. Closest to our setting, SCARED formulates safe ICRL under CMDPs and learns budget-sensitive policies through Lagrangian pretraining without test-time parameter updates [40]. Our method focuses on a deployment-time gap: with a fixed pretrained ICRL policy, action selection may still place probability on actions whose predicted future cost exceeds the remaining budget. We therefore add a runtime barrier that reweights candidate actions using the current latent context, remaining budget, and predicted cumulative cost.

**Latent Representations, Safety Filters, and Auxiliary Training.** Our shield relies on latent representations that support policy adaptation, latent dynamics prediction, and safety estimation. Prior work on context encoders, function encoders, and world-model representations shows that learned latent variables can capture task or dynamics information useful for zero-shot transfer, in-context adaptation, and hidden-parameter generalization [37, 23, 22, 43, 29, 31]. Closely related to our runtime safety mechanism, recent latent safety-filter methods perform safety analysis directly in learned world-model spaces using latent reachability, uncertainty-aware filtering, or runtime-adaptive safety constraints [41, 50, 2]. These works provide important precedent for latent-space runtime safety reasoning, but our mechanism differs: we use a CMDP-style remaining budget, a world-projected latent state, one-step latent dynamics, and a pessimistic cost-to-go critic to define a latent Q-barrier for candidate-action reweighting. Finally, our training objective uses auxiliary dynamics and safety losses to shape the representation. Auxiliary prediction objectives are widely used to improve RL representations [24, 32, 49, 70] but joint policy, dynamics, and safety optimization can create gradient interference. To reduce this interference, we use an asymmetric stop-gradient scheme inspired by self-supervised representation learning methods such as BYOL, where prediction heads are trained against target representations while gradients are selectively blocked [19]. In our setting, grounding losses update the shared encoder, while alignment losses pass through projection heads with stop-gradient, allowing auxiliary supervision to regularize the latent space without directly destabilizing policy learning.

## 7 Conclusion

We introduced Q-Barrier, a latent shielding mechanism that makes frozen safe ICRL policies explicitly budget-aware under test-time generalization shifts, including both structural OOD and unseen ID settings. The method augments a safe ICRL policy with shield-supporting modules learned during training: a world-projected latent representation, a latent dynamics model, and a cost-critic ensemble. At deployment, all learned parameters remain fixed, and Q-Barrier only reweights finite action candidates using the remaining budget and predicted cost-to-go, so adaptation comes from the growing in-context history rather than online parameter updates.

Our analysis shows that an action with sufficient Q-Barrier margin preserves an approximate next-step budget-safe continuation over the next candidate set, up to Bellman upper bound and latent prediction errors. Empirically, Q-Barrier improves reward-safety tradeoffs during test-time in-context adaptation. After a short context window, it achieves higher return in four of five environments while

matching or lowering average episode cost in all five, with one environment showing a conservative lower-cost/lower-return tradeoff. Across budget sweeps, it achieves the highest return in four of five environments while generally matching or reducing average cost relative to baselines.

**Limitations and future work.** Q-Barrier depends on latent prediction accuracy, critic calibration, Bellman residuals, and sampled candidate quality. Overly pessimistic cost estimates can downweight useful high-return actions. Future work should improve uncertainty calibration, adapt shield strength to local uncertainty and remaining budget, extend to multiple constraints, and develop stronger closed-loop analyses for stochastic shielded policies.

## References

- [1] Joshua Achiam, David Held, Aviv Tamar, and Pieter Abbeel. Constrained policy optimization. In *Proceedings of the International Conference on Machine Learning*, 2017.
- [2] Sankalp Agrawal, Junwon Seo, Kensuke Nakamura, Ran Tian, and Andrea Bajcsy. Anysafe: Adapting latent safety filters at runtime via safety constraint parameterization in the latent space. *IEEE International Conference on Robotics and Automation (ICRA)*, 2026.
- [3] Mohammed Alshiekh, Roderick Bloem, Rüdiger Ehlers, Bettina Könighofer, Scott Niekum, and Ufuk Topcu. Safe reinforcement learning via shielding. In *AAAI Conference on Artificial Intelligence*, 2018.
- [4] Eitan Altman. *Constrained Markov decision processes*. Routledge, 2021.
- [5] Yarden As, Bhavya Sukhija, Lenart Treven, Carmelo Sferrazza, Stelian Coros, and Andreas Krause. Actsafes: Active exploration with safety constraints for reinforcement learning. In *The Thirteenth International Conference on Learning Representations*, 2025.
- [6] Carolin Benjamins, Theresa Eimer, Frederik Schubert, Aditya Mohan, Sebastian Döhler, André Biedenkapp, Bodo Rosenhahn, Frank Hutter, and Marius Lindauer. Contextualize me – the case for context in reinforcement learning. *Transactions on Machine Learning Research*, 2023.
- [7] Steven Carr, Nils Jansen, Sebastian Junges, and Ufuk Topcu. Safe reinforcement learning via shielding under partial observability. In *The Thirty-Seventh AAAI Conference on Artificial Intelligence*, 2023.
- [8] Baiming Chen, Zuxin Liu, Jiacheng Zhu, Mengdi Xu, Wenhao Ding, Liang Li, and Ding Zhao. Context-aware safe reinforcement learning for non-stationary environments. In *2021 IEEE International Conference on Robotics and Automation (ICRA)*, 2021.
- [9] Xiaoyu Chen, Xiangming Zhu, Yufeng Zheng, Pushi Zhang, Li Zhao, Wenxue Cheng, Peng Cheng, Yongqiang Xiong, Tao Qin, Jianyu Chen, and Tie-Yan Liu. An adaptive deep RL method for non-stationary environments with piecewise stable context. In *Advances in Neural Information Processing Systems*, 2022.
- [10] Yikun Cheng, Pan Zhao, and Naira Hovakimyan. Safe and efficient reinforcement learning using disturbance-observer-based control barrier functions. In *Proceedings of The 5th Annual Learning for Dynamics and Control Conference*, 2023.
- [11] Jason Choi, Fernando Castañeda, Claire J. Tomlin, and Koushil Sreenath. Reinforcement learning for safety-critical control under model uncertainty, using control lyapunov functions and control barrier functions. In *Robotics: Science and Systems*, 2020.
- [12] Zhenwen Dai, Federico Tomasi, and Sina Ghiassian. In-context exploration-exploitation for reinforcement learning. *ArXiv Preprint*, 2024.
- [13] Juncheng Dong, Moyang Guo, Ethan X. Fang, Zhuoran Yang, and Vahid Tarokh. In-context reinforcement learning without optimal action labels. In *ICML 2024 Workshop on In-Context Learning*, 2024.
- [14] Yan Duan, John Schulman, Xi Chen, Peter L Bartlett, Ilya Sutskever, and Pieter Abbeel. RL<sup>2</sup>: Fast reinforcement learning via slow reinforcement learning. *ArXiv Preprint*, 2016.

- [15] Chelsea Finn, Pieter Abbeel, and Sergey Levine. Model-agnostic meta-learning for fast adaptation of deep networks. In *Proceedings of the International Conference on Machine Learning*, 2017.
- [16] Milan Ganai, Zheng Gong, Chenning Yu, Sylvia Lee Herbert, and Sicun Gao. Iterative reachability estimation for safe reinforcement learning. In *Thirty-seventh Conference on Neural Information Processing Systems*, 2023.
- [17] Jake Grigsby, Linxi Fan, and Yuke Zhu. Amago: Scalable in-context reinforcement learning for adaptive agents. In *Proceedings of the International Conference on Learning Representations*, 2024.
- [18] Jake Grigsby, Justin Sasek, Samyak Parajuli, Ikechukwu D Adebisi, Amy Zhang, and Yuke Zhu. Amago-2: Breaking the multi-task barrier in meta-reinforcement learning with transformers. In *Advances in Neural Information Processing Systems*, 2024.
- [19] Jean-Bastien Grill, Florian Strub, Florent Altché, Corentin Tallec, Pierre H. Richemond, Elena Buchatskaya, Carl Doersch, Bernardo Avila Pires, Zhaohan Daniel Guo, Mohammad Gheshlaghi Azar, Bilal Piot, Koray Kavukcuoglu, Rémi Munos, and Michal Valko. Bootstrap your own latent: a new approach to self-supervised learning. In *Proceedings of the 34th International Conference on Neural Information Processing Systems*, 2020.
- [20] Shangding Gu, Laixi Shi, Yuhao Ding, Alois Knoll, Costas Spanos, Adam Wierman, and Ming Jin. Enhancing efficiency of safe reinforcement learning via sample manipulation. In *The Thirty-eighth Annual Conference on Neural Information Processing Systems*, 2024.
- [21] Cong Guan, Ruiqi Xue, Ziqian Zhang, Lihe Li, Yi-Chen Li, Lei Yuan, and Yang Yu. Cost-aware offline safe meta reinforcement learning with robust in-distribution online task adaptation. In *Proceedings of the International Conference on Autonomous Agents and Multiagent Systems*, 2024.
- [22] Tyler Ingebrand, Adam Thorpe, and Ufuk Topcu. Zero-shot transfer of neural ODEs. In *The Thirty-eighth Annual Conference on Neural Information Processing Systems*, 2024.
- [23] Tyler Ingebrand, Amy Zhang, and Ufuk Topcu. Zero-shot reinforcement learning via function encoders. In *Proceedings of the 41st International Conference on Machine Learning*, 2024.
- [24] Max Jaderberg, Volodymyr Mnih, Wojciech Marian Czarnecki, Tom Schaul, Joel Z Leibo, David Silver, and Koray Kavukcuoglu. Reinforcement learning with unsupervised auxiliary tasks. In *International Conference on Learning Representations*, 2017.
- [25] Jiaming Ji, Borong Zhang, Jiayi Zhou, Xuehai Pan, Weidong Huang, Ruiyang Sun, Yiran Geng, Yifan Zhong, Josef Dai, and Yaodong Yang. Safety gymnasium: A unified safe reinforcement learning benchmark. In *Advances in Neural Information Processing Systems*, 2023.
- [26] Vanshaj Khattar, Yuhao Ding, Bilgehan Sel, Javad Lavaei, and Ming Jin. A CMDP-within-online framework for meta-safe reinforcement learning. In *Proceedings of the International Conference on Learning Representations*, 2023.
- [27] Robert Kirk, Amy Zhang, Edward Grefenstette, and Tim Rocktäschel. A survey of zero-shot generalisation in deep reinforcement learning. *ArXiv Preprint*, 2021.
- [28] Louis Kirsch, James Harrison, C. Freeman, Jascha Sohl-Dickstein, and Jürgen Schmidhuber. Towards general-purpose in-context learning agents. In *NeurIPS Foundation Models for Decision Making Workshop*, 2023.
- [29] Cevahir Koprulu, Thiago D. Simão, Nils Jansen, and Ufuk Topcu. Safety-prioritizing curricula for constrained reinforcement learning. In *The Thirteenth International Conference on Learning Representations*, 2025.
- [30] Akshay Krishnamurthy, Keegan Harris, Dylan J Foster, Cyril Zhang, and Aleksandrs Slivkins. Can large language models explore in-context? *ArXiv Preprint*, 2024.

- [31] Minjae Kwon, Tyler Ingebrand, Ufuk Topcu, and Lu Feng. Adaptive shielding for safe reinforcement learning under hidden-parameter dynamics shifts, 2026. URL <https://arxiv.org/abs/2506.11033>.
- [32] Michael Laskin, Aravind Srinivas, and Pieter Abbeel. Curl: Contrastive unsupervised representations for reinforcement learning. In *Proceedings of the International Conference on Machine Learning*, 2020.
- [33] Michael Laskin, Luyu Wang, Junhyuk Oh, Emilio Parisotto, Stephen Spencer, Richie Steigerwald, DJ Strouse, Steven Stenberg Hansen, Angelos Filos, Ethan Brooks, Maxime Gazeau, Himanshu Sahni, Satinder Singh, and Volodymyr Mnih. In-context reinforcement learning with algorithm distillation. In *Proceedings of the International Conference on Learning Representations*, 2023.
- [34] Jonathan Lee, Annie Xie, Aldo Pacchiano, Yash Chandak, Chelsea Finn, Ofir Nachum, and Emma Brunskill. Supervised pretraining can learn in-context reinforcement learning. In *Advances in Neural Information Processing Systems*, 2023.
- [35] Lars Lindemann, Matthew Cleaveland, Gihyun Shim, and George J. Pappas. Safe planning in dynamic environments using conformal prediction. *IEEE Robotics and Automation Letters*, 2023.
- [36] Jinmei Liu, Fuhong Liu, Zhenhong Sun, Jianye HAO, Huaxiong Li, Bo Wang, Daoyi Dong, Chunlin Chen, and Zhi Wang. Scalable in-context q-learning. In *The Fourteenth International Conference on Learning Representations*, 2026.
- [37] Fan-Ming Luo, Shengyi Jiang, Yang Yu, ZongZhang Zhang, and Yi-Feng Zhang. Adapt to environment sudden changes by learning a context-sensitive policy. In *Proceedings of the AAAI Conference on Artificial Intelligence*, 2022.
- [38] Michael Luo, Ashwin Balakrishna, Brijen Thananjeyan, Suraj Nair, Julian Ibarz, Jie Tan, Chelsea Finn, Ion Stoica, and Ken Goldberg. Mesa: Offline meta-rl for safe adaptation and fault tolerance. In *Advances in Neural Information Processing Systems*, 2021.
- [39] Amir Moeini, Jiuqi Wang, Jacob Beck, Ethan Blaser, Shimon Whiteson, Rohan Chandra, and Shangtong Zhang. A survey of in-context reinforcement learning. *ArXiv Preprint*, 2025.
- [40] Amir Moeini, Minjae Kwon, Alper Kamil Bozkurt, Yuichi Motai, Rohan Chandra, Lu Feng, and Shangtong Zhang. Safe in-context reinforcement learning. In *International Conference on Machine Learning (ICML)*, 2026.
- [41] Kensuke Nakamura, Lasse Peters, and Andrea Bajcsy. Generalizing safety beyond collision-avoidance via latent-space reachability analysis. In *Robotics: Science and Systems XXI*, 2025.
- [42] Andrei Polubarov, Lyubaykin Nikita, Alexander Derevyagin, Ilya Zisman, Denis Tarasov, Alexander Nikulin, and Vladislav Kurenkov. Vintix: Action model via in-context reinforcement learning. In *Forty-second International Conference on Machine Learning*, 2025.
- [43] Sai Prasanna, Karim Farid, Raghu Rajan, and André Biedenkapp. Dreaming of many worlds: Learning contextual world models aids zero-shot generalization. *Reinforcement Learning Journal*, 2024.
- [44] Martin L Puterman. *Markov decision processes: discrete stochastic dynamic programming*. John Wiley & Sons, 2014.
- [45] Sharath Chandra Raparthi, Eric Hambro, Robert Kirk, Mikael Henaff, and Roberta Raileanu. Generalization to new sequential decision making tasks with in-context learning. *ArXiv Preprint*, 2023.
- [46] Alex Ray, Joshua Achiam, and Dario Amodei. Benchmarking safe exploration in deep reinforcement learning. *OpenAI*. <https://cdn.openai.com/safexp-short.pdf>, 2019.
- [47] William Scarbro, Calum Imrie, Sinem Getir Yaman, Kavan Fatehi, Corina Păsăreanu, Radu Calinescu, and Ravi Mangal. Conformal safety shielding for imperfect-perception agents. In *International Conference on Runtime Verification*, 2025.

- [48] John Schulman, Filip Wolski, Prafulla Dhariwal, Alec Radford, and Oleg Klimov. Proximal policy optimization algorithms. *ArXiv Preprint*, 2017.
- [49] Max Schwarzer, Nitarshan Rajkumar, Michael Noukhovitch, Ankesh Anand, Laurent Charlin, R Devon Hjelm, Philip Bachman, and Aaron Courville. Pretraining representations for data-efficient reinforcement learning. In A. Beygelzimer, Y. Dauphin, P. Liang, and J. Wortman Vaughan, editors, *Advances in Neural Information Processing Systems*, 2021.
- [50] Junwon Seo, Kensuke Nakamura, and Andrea Bajcsy. Uncertainty-aware latent safety filters for avoiding out-of-distribution failures. *Conference on Robot Learning (CoRL)*, 2025.
- [51] Shili Sheng, David Parker, and Lu Feng. Safe pomdp online planning via shielding. In *2024 IEEE International Conference on Robotics and Automation*, 2024.
- [52] Shili Sheng, Pian Yu, David Parker, Marta Kwiatkowska, and Lu Feng. Safe pomdp online planning among dynamic agents via adaptive conformal prediction. *IEEE Robotics and Automation Letters*, 2024.
- [53] Viacheslav Sini, Alexander Nikulin, Vladislav Kurenkov, Ilya Zisman, and Sergey Kolesnikov. In-context reinforcement learning for variable action spaces. In *Forty-first International Conference on Machine Learning*, 2024.
- [54] Jaehyeon Son, Soochan Lee, and Gunhee Kim. Distilling reinforcement learning algorithms for in-context model-based planning. In *Proceedings of the International Conference on Learning Representations*, 2025.
- [55] Richard S Sutton and Andrew G Barto. *Reinforcement Learning: An Introduction (2nd Edition)*. MIT Press, 2018.
- [56] Emanuel Todorov, Tom Erez, and Yuval Tassa. Mujoco: A physics engine for model-based control. In *Proceedings of the International Conference on Intelligent Robots and Systems*, 2012.
- [57] Akifumi Wachi and Yanan Sui. Safe reinforcement learning in constrained markov decision processes. In *Proceedings of the International Conference on Machine Learning*, 2020.
- [58] Jane X Wang, Zeb Kurth-Nelson, Dhruva Tirumala, Hubert Soyer, Joel Z Leibo, Remi Munos, Charles Blundell, Dharshan Kumaran, and Matt Botvinick. Learning to reinforcement learn. *ArXiv Preprint*, 2016.
- [59] Jiuqi Wang, Ethan Blaser, Hadi Daneshmand, and Shangdong Zhang. Transformers can learn temporal difference methods for in-context reinforcement learning. In *Proceedings of the International Conference on Learning Representations*, 2025.
- [60] Jiuqi Wang, Rohan Chandra, and Shangdong Zhang. Towards provable emergence of in-context reinforcement learning. In *Advances in Neural Information Processing Systems*, 2025.
- [61] Yixuan Wang, Simon Sinong Zhan, Ruochen Jiao, Zhilu Wang, Wanxin Jin, Zhuoran Yang, Zhaoran Wang, Chao Huang, and Qi Zhu. Enforcing hard constraints with soft barriers: Safe reinforcement learning in unknown stochastic environments. In *Proceedings of the 40th International Conference on Machine Learning*, 2023.
- [62] Wei Xiao, Tsun-Hsuan Wang, Ramin Hasani, Makram Chahine, Alexander Amini, Xiao Li, and Daniela Rus. Barriernet: Differentiable control barrier functions for learning of safe robot control. *IEEE Transactions on Robotics*, 2023.
- [63] Mengdi Xu, Yikang Shen, Shun Zhang, Yuchen Lu, Ding Zhao, Joshua Tenenbaum, and Chuang Gan. Prompting decision transformer for few-shot policy generalization. In *Proceedings of the International Conference on Machine Learning*, 2022.
- [64] Siyuan Xu and Minghui Zhu. Efficient safe meta-reinforcement learning: Provable near-optimality and anytime safety. In *Advances in Neural Information Processing Systems*, 2025.

- [65] Jiachen Yang, Brenden Petersen, Hongyuan Zha, and Daniel Faissol. Single episode policy transfer in reinforcement learning. In *International Conference on Learning Representations*, 2020.
- [66] Long Yang, Jiaming Ji, Juntao Dai, Linrui Zhang, Binbin Zhou, Pengfei Li, Yaodong Yang, and Gang Pan. Constrained update projection approach to safe policy optimization. In *Advances in Neural Information Processing Systems*, 2022.
- [67] Tsung-Yen Yang, Justinian Rosca, Karthik Narasimhan, and Peter J. Ramadge. Projection-based constrained policy optimization. In *International Conference on Learning Representations*, 2020.
- [68] Wen-Chi Yang, Giuseppe Marra, Gavin Rens, and Luc De Raedt. Safe reinforcement learning via probabilistic logic shields. In *Proceedings of the Thirty-Second International Joint Conference on Artificial Intelligence, IJCAI-23*, 2023.
- [69] Yiming Zhang, Quan Vuong, and Keith W. Ross. First order constrained optimization in policy space. In *Proceedings of the 34th International Conference on Neural Information Processing Systems*, 2020.
- [70] Yi Zhao, Wenshuai Zhao, Rinu Boney, Juho Kannala, and Joni Pajarinen. Simplified temporal consistency reinforcement learning. In *Proceedings of the 40th International Conference on Machine Learning*, 2023.
- [71] Ilya Zisman, Vladislav Kurenkov, Alexander Nikulin, Viacheslav Sinii, and Sergey Kolesnikov. Emergence of in-context reinforcement learning from noise distillation. *ArXiv Preprint*, 2023.

## A Proofs

### A.1 Proof of Theorem 1

Before proving the main theorem, we first prove a value error lemma. Under Assumptions 1 and 2, the lemma shows that latent prediction error can change the estimated next-step continuation value by at most  $L_Q \varepsilon_{\text{pred}}$ .

**Lemma 1.** *Under Assumptions 1 and 2,*

$$\left| \hat{V}_{C,t+1}^{+,k}(f_z(Z_t^{w,k}, A_t^k)) - \hat{V}_{C,t+1}^{+,k}(Z_{t+1}^{w,k}) \right| \leq L_Q \varepsilon_{\text{pred}}. \quad (7)$$

*Proof.* Fix episode  $k$  and timestep  $t$ , and condition on the realized next-step candidate set  $\mathcal{A}_{t+1,k}^{\text{cand}}$ . Write  $\hat{V}_C^+(Z) \doteq \hat{V}_{C,t+1}^{+,k}(Z) = \min_{A' \in \mathcal{A}_{t+1,k}^{\text{cand}}} \hat{Q}_C^+(Z, A')$ . For readability, we omit  $+$  and  $k$  in intermediate expressions when there is no ambiguity. Since  $\mathcal{A}_{t+1,k}^{\text{cand}}$  is fixed in this argument and each function  $\hat{Q}_C^+(\cdot, A')$  is  $L_Q$ -Lipschitz, their pointwise minimum is also  $L_Q$ -Lipschitz. To see this, let  $A^* \in \arg \min_{A' \in \mathcal{A}_{t+1,k}^{\text{cand}}} \hat{Q}_C^+(Z', A')$ . Then  $\hat{V}_C^+(Z) - \hat{V}_C^+(Z') \leq \hat{Q}_C^+(Z, A^*) - \hat{Q}_C^+(Z', A^*) \leq L_Q \|Z - Z'\|_2$ . Swapping  $Z$  and  $Z'$  leads to  $|\hat{V}_C^+(Z) - \hat{V}_C^+(Z')| \leq L_Q \|Z - Z'\|_2$ . Applying this bound with  $Z = f_z(Z_t^{w,k}, A_t^k)$  and  $Z' = Z_{t+1}^{w,k}$ , and using Assumption 1, proves Equation (7).  $\square$

*Proof.* Fix episode  $k$  and timestep  $t$ , and condition on the realized next-step candidate set  $\mathcal{A}_{t+1,k}^{\text{cand}}$ . We follow the same convention used in Proof of Lemma 1.

Starting from the next-step state barrier and using the budget recursion  $B_{t+1}^k = B_t^k - C_{t+1}^k$ , we have

$$\begin{aligned}
b_{V,t+1}^k(Z_{t+1}^{w,k}, B_{t+1}^k) &= B_{t+1}^k - \hat{V}_C^+(Z_{t+1}^{w,k}) \\
&= B_t^k - C_{t+1}^k - \hat{V}_C^+(Z_{t+1}^{w,k}) \\
&= \underbrace{B_t^k - \hat{Q}_C^+(Z_t^{w,k}, A_t^k)}_{b_{Q,t}^k(Z_t^{w,k}, B_t^k, A_t^k)} \\
&\quad + \left( \hat{Q}_C^+(Z_t^{w,k}, A_t^k) - C_{t+1}^k - \hat{V}_C^+(f_z(Z_t^{w,k}, A_t^k)) \right) \\
&\quad + \left( \hat{V}_C^+(f_z(Z_t^{w,k}, A_t^k)) - \hat{V}_C^+(Z_{t+1}^{w,k}) \right).
\end{aligned}$$

By the definition of the Bellman upper-bound residual,

$$\hat{Q}_C^+(Z_t^{w,k}, A_t^k) - C_{t+1}^k - \hat{V}_C^+(f_z(Z_t^{w,k}, A_t^k)) \geq -\Delta_{\text{bell},t}^{+,k}.$$

By Lemma 1,  $\hat{V}_C^+(f_z(Z_t^{w,k}, A_t^k)) - \hat{V}_C^+(Z_{t+1}^{w,k}) \geq -L_Q \varepsilon_{\text{pred}}$ . Substituting both inequalities gives

$$b_{V,t+1}^k(Z_{t+1}^{w,k}, B_{t+1}^k) \geq b_{Q,t}^k(Z_t^{w,k}, B_t^k, A_t^k) - \Delta_{\text{bell},t}^{+,k} - L_Q \varepsilon_{\text{pred}},$$

which proves the claim.  $\square$

## A.2 Episode-Level Budget Bound

Theorem 1 is a one-step result. This subsection shows that it can be extended into an episode-level bound on cumulative budget accumulation by introducing a term that captures the gap between the action actually selected and the critic-minimizing action.

**Definition 3** (Selection Gap). *For the action selected at time  $t$  in episode  $k$ , define*

$$\Delta_{\text{sel},t}^k \doteq \hat{Q}_C^+(Z_t^{w,k}, A_t^k) - \hat{V}_{C,t}^{+,k}(Z_t^{w,k}) \geq 0. \quad (8)$$

This quantity is the excess predicted cost-to-go of the selected action over the minimum available in the candidate set at that state. It is zero when the deployed policy selects the critic-minimizing action, and positive when stochastic shielding picks a higher-cost action. Recall that

$$b_{V,t}^k(Z, B) \doteq B - \hat{V}_{C,t}^{+,k}(Z), \quad b_{Q,t}^k(Z, B, A) \doteq B - \hat{Q}_C^+(Z, A).$$

For continuous-action environments, all quantities are conditioned on the realized finite candidate sets. The candidate set  $\mathcal{A}_{t+1,k}^{\text{cand}}$  used in the Bellman residual at time  $t$  is the same candidate set used to define  $b_{V,t+1}^k$  at the next decision making. We assume that each realized candidate set is nonempty and that the executed action  $A_t^k$  is selected from  $\mathcal{A}_{t,k}^{\text{cand}}$ . Thus  $\Delta_{\text{sel},t}^k \geq 0$ . In continuous-action domains, the proposition is conditional on the entire realized sequence of finite candidate sets.

**Proposition 1** (Episode-Level Budget Bound). *Suppose Theorem 1 holds along episode  $k$  with the signed budget recursion  $B_{t+1}^k = B_t^k - C_{t+1}^k$ . Assume the terminal condition  $\hat{V}_{C,T_k}^{+,k}(Z_{T_k}^{w,k}) = 0$ . Then*

$$G_{c,0}(\tau_k) - B_0^k \leq -b_{V,0}^k(Z_0^{w,k}, B_0^k) + \sum_{t=0}^{T_k-1} \left( \Delta_{\text{sel},t}^k + \Delta_{\text{bell},t}^{+,k} + L_Q \varepsilon_{\text{pred}} \right). \quad (9)$$

In particular, if  $B_0^k = \delta$  and  $b_{V,0}^k(Z_0^{w,k}, \delta) \geq 0$ , then

$$G_{c,0}(\tau_k) - \delta \leq \sum_{t=0}^{T_k-1} \left( \Delta_{\text{sel},t}^k + \Delta_{\text{bell},t}^{+,k} + L_Q \varepsilon_{\text{pred}} \right). \quad (10)$$

Averaging over  $K$  episodes and taking expectation gives

$$\frac{1}{K} \sum_{k=1}^K \mathbb{E}[G_{c,0}(\tau_k)] \leq \delta + \frac{1}{K} \sum_{k=1}^K \mathbb{E} \left[ \sum_{t=0}^{T_k-1} \left( \Delta_{\text{sel},t}^k + \Delta_{\text{bell},t}^{+,k} + L_Q \varepsilon_{\text{pred}} \right) - b_{V,0}^k(Z_0^{w,k}, \delta) \right]. \quad (11)$$

*Proof.* By the definition of the selection gap,

$$\Delta_{\text{sel},t}^k = \hat{Q}_C^+(Z_t^{w,k}, A_t^k) - \hat{V}_{C,t}^{+,k}(Z_t^{w,k}).$$

Therefore,

$$\begin{aligned} b_{Q,t}^k(Z_t^{w,k}, B_t^k, A_t^k) &= B_t^k - \hat{Q}_C^+(Z_t^{w,k}, A_t^k) \\ &= B_t^k - \hat{V}_{C,t}^{+,k}(Z_t^{w,k}) - \Delta_{\text{sel},t}^k \\ &= b_{V,t}^k(Z_t^{w,k}, B_t^k) - \Delta_{\text{sel},t}^k. \end{aligned}$$

Substituting this identity into Theorem 1 gives

$$b_{V,t+1}^k(Z_{t+1}^{w,k}, B_{t+1}^k) \geq b_{V,t}^k(Z_t^{w,k}, B_t^k) - \Delta_{\text{sel},t}^k - \Delta_{\text{bell},t}^{+,k} - L_Q \varepsilon_{\text{pred}}. \quad (12)$$

Summing Equation (12) over  $t = 0, \dots, T_k - 1$  and telescoping provides

$$b_{V,T_k}^k(Z_{T_k}^{w,k}, B_{T_k}^k) \geq b_{V,0}^k(Z_0^{w,k}, B_0^k) - \sum_{t=0}^{T_k-1} \left( \Delta_{\text{sel},t}^k + \Delta_{\text{bell},t}^{+,k} + L_Q \varepsilon_{\text{pred}} \right).$$

By the terminal condition  $\hat{V}_{C,T_k}^{+,k}(Z_{T_k}^{w,k}) = 0$ , we have

$$b_{V,T_k}^k(Z_{T_k}^{w,k}, B_{T_k}^k) = B_{T_k}^k.$$

Using the budget identity

$$B_{T_k}^k = B_0^k - G_{c,0}(\tau_k),$$

we obtain

$$B_0^k - G_{c,0}(\tau_k) \geq b_{V,0}^k(Z_0^{w,k}, B_0^k) - \sum_{t=0}^{T_k-1} \left( \Delta_{\text{sel},t}^k + \Delta_{\text{bell},t}^{+,k} + L_Q \varepsilon_{\text{pred}} \right).$$

Finally, rearranging gives Equation (9). Setting  $B_0^k = \delta$  and using  $b_{V,0}^k(Z_0^{w,k}, \delta) \geq 0$  gives Equation (10). Averaging Equation (9) over  $k$  and taking expectations gives Equation (11).  $\square$

**Remark.** Proposition 1 connects the local one-step barrier analysis to the aggregate budget objective through the selection gap  $\Delta_{\text{sel},t}^k$ , which measures how much the chosen action's predicted cost exceeds the lowest predicted cost among candidates. For the soft shield, this term captures the cost of preserving policy support rather than always selecting the critic-greedy lowest-cost action. The result does not by itself guarantee  $\frac{1}{K} \sum_k \mathbb{E}[G_{c,0}(\tau_k)] \leq \delta$ . Instead, it decomposes episode-level budget into measurable residuals from action selection, critic conservatism, and latent prediction error.

### A.3 Overlap of Consecutive Safe Sets

The following result gives a local interpretation of the Lipschitz regularity assumption. Since candidate sets may be resampled over time, the statement is conditional on an action being present in both consecutive candidate sets.

**Definition 4** (Safe Candidate Set). *For the realized candidate set  $\mathcal{A}_{t,k}^{\text{cand}}$ , world-projected latent state  $Z \in \mathcal{Z}^w$ , and remaining budget  $B$ , define*

$$\mathcal{A}_{\text{safe},t}^k(Z, B) \doteq \left\{ A \in \mathcal{A}_{t,k}^{\text{cand}} : \hat{Q}_C^+(Z, A) \leq B \right\}. \quad (13)$$

**Lemma 2** (Conditional Overlap of Consecutive Safe Candidate Sets). *Suppose Assumption 2 holds. Let  $A \in \mathcal{A}_{t,k}^{\text{cand}} \cap \mathcal{A}_{t+1,k}^{\text{cand}}$  satisfy*

$$\hat{Q}_C^+(Z_t^{w,k}, A) \leq B_t^k - \eta \quad (14)$$

for some margin  $\eta > 0$ . If

$$L_Q \|Z_{t+1}^{w,k} - Z_t^{w,k}\|_2 + |B_{t+1}^k - B_t^k| \leq \eta, \quad (15)$$

then

$$A \in \mathcal{A}_{\text{safe},t+1}^k(Z_{t+1}^{w,k}, B_{t+1}^k). \quad (16)$$

Consequently, if such an action exists, then

$$\mathcal{A}_{\text{safe},t}^k(Z_t^{w,k}, B_t^k) \cap \mathcal{A}_{\text{safe},t+1}^k(Z_{t+1}^{w,k}, B_{t+1}^k) \neq \emptyset. \quad (17)$$

*Proof.* Because  $A \in \mathcal{A}_{t,k}^{\text{cand}} \cap \mathcal{A}_{t+1,k}^{\text{cand}}$ , it is eligible at both consecutive decision times. By Assumption 2,

$$|\hat{Q}_C^+(Z_{t+1}^{w,k}, A) - \hat{Q}_C^+(Z_t^{w,k}, A)| \leq L_Q \|Z_{t+1}^{w,k} - Z_t^{w,k}\|_2.$$

Using Equation (14), we have

$$\hat{Q}_C^+(Z_{t+1}^{w,k}, A) \leq B_t^k - \eta + L_Q \|Z_{t+1}^{w,k} - Z_t^{w,k}\|_2.$$

Therefore,

$$\hat{Q}_C^+(Z_{t+1}^{w,k}, A) - B_{t+1}^k \leq L_Q \|Z_{t+1}^{w,k} - Z_t^{w,k}\|_2 - \eta + |B_{t+1}^k - B_t^k|.$$

By Equation (15), the right-hand side is less or equal than 0, so

$$\hat{Q}_C^+(Z_{t+1}^{w,k}, A) \leq B_{t+1}^k.$$

Since  $A \in \mathcal{A}_{t+1,k}^{\text{cand}}$ , this implies  $A \in \mathcal{A}_{\text{safe},t+1}^k(Z_{t+1}^{w,k}, B_{t+1}^k)$ . The overlap claim follows because Equation (14) also implies  $A \in \mathcal{A}_{\text{safe},t}^k(Z_t^{w,k}, B_t^k)$ .  $\square$

This overlap result is mainly relevant for discrete action spaces or continuous implementations that reuse candidate actions across consecutive steps. With independent continuous resampling, the exact overlap condition is less likely to hold.

#### A.4 Pessimistic Ensemble Cost Critics

This section describes how the ensemble cost critics are trained and how the pessimistic ensemble estimate used by the Q-barrier relates to the Bellman upper-bound error  $\Delta_{\text{bell},t}^{+,k}$  in Equation (6).

**Cost-value target.** We do not parameterize the cost value by a separate value network. Instead, the target value is induced by the target cost-Q ensemble. For each transition, we sample  $K_c$  next actions from the target policy,  $a'_\ell \sim \pi_{\bar{\theta}}(\cdot | Z_{t+1}^{p,k})$ ,  $\ell = 1, \dots, K_c$ . We define the pessimistic target cost value as  $\hat{V}_C(Z_{t+1}^{w,k}) = \frac{1}{K_c} \sum_{\ell=1}^{K_c} \bar{Q}_{C,j}(Z_{t+1}^{w,k}, a'_\ell)$ , where  $\bar{Q}_{C,j}$  denotes the target network for critic head  $j$ . The resulting cost Bellman target is  $Y_t^C = C_{t+1} + (1 - d_{t+1}^{\text{ctx}}) \hat{V}_C(Z_{t+1}^{w,k})$ , where  $d_{t+1}^{\text{ctx}}$  indicates an in-context episode boundary. The target is computed using target networks and is detached from the critic update.

**Critic training.** We train an ensemble of  $M$  online cost critics  $\{\hat{Q}_{C,i}\}_{i=1}^M$  by regressing each head to the same detached target:  $\mathcal{L}_{Q_C} = \mathbb{E}_{i,t} \left[ \left( \hat{Q}_{C,i}(Z_t^{w,k}, A_t^k) - Y_t^C \right)^2 \right]$ . Thus, the loss is averaged over critic heads, while pessimism enters through the detached target construction rather than through a direct maximization over online critic predictions. In our experiments, we use  $M = 4$  cost critics, and  $K_c = 1$ . Hence the target reduces to the maximum over two randomly selected target critics evaluated at one target-policy action.

**Runtime pessimism.** At action selection time, the Q-barrier uses the ensemble maximum  $\hat{Q}_C^+(Z_t^{w,k}, A) \doteq \max_{i \in \{1, \dots, M\}} \hat{Q}_{C,i}(Z_t^{w,k}, A)$ . The barrier margin is then computed as  $b_{Q,t}^k(Z_t^{w,k}, B_t^k, A) = B_t^k - \hat{Q}_C^+(Z_t^{w,k}, A)$ . This worst-case aggregation makes the shield conservative when critic heads disagree, reducing the chance that an action is treated as safe because of a single underestimated cost prediction.

**Effect on  $\Delta_{\text{bell},t}^k$ .** The pessimistic ensemble is a deployment-time heuristic intended to reduce  $\Delta_{\text{bell},t}^k$  empirically by biasing cost estimates conservatively in states where critic disagreement is large. We do not claim that it enforces Bellman conservatism theoretically. Instead, the role of the ensemble maximum is to make underestimation less likely in uncertain states, while its actual effect on  $\Delta_{\text{bell},t}^k$  is evaluated through Bellman-error diagnostics in Section 5. Accordingly, this decoupled strategy may reduce the Bellman upper-bound error in practice, but it does not guarantee  $\Delta_{\text{bell},t}^k = 0$ .

Environment	$\epsilon_{\text{pred}} \downarrow$	$e_V^+ \downarrow$	$\widehat{L}_Q^{\text{local},+} \downarrow$	Bellman sat. $\widehat{Q}_C^+ \uparrow$	$\Delta_{\text{bell}}^+ \downarrow$
SafeDarkRoom	0.00252 $\pm$ 0.00002	0.3595 $\pm$ 0.0056	228.8 $\pm$ 3.0	72.2 $\pm$ 1.0	67.19 $\pm$ 3.20
SafeDarkMujoco-Point	0.00766 $\pm$ 0.00056	0.0847 $\pm$ 0.0053	14.10 $\pm$ 0.22	89.8 $\pm$ 0.9	0.248 $\pm$ 0.048
SafeDarkMujoco-Car	0.00906 $\pm$ 0.00058	0.0972 $\pm$ 0.0061	13.08 $\pm$ 0.14	89.8 $\pm$ 0.4	0.104 $\pm$ 0.004
SafeVelocity-HalfCheetah	0.0460 $\pm$ 0.0008	0.0432 $\pm$ 0.0009	0.872 $\pm$ 0.003	70.5 $\pm$ 0.2	0.386 $\pm$ 0.005
SafeVelocity-Ant	0.00478 $\pm$ 0.00013	0.0514 $\pm$ 0.0019	10.35 $\pm$ 0.14	89.9 $\pm$ 0.5	0.719 $\pm$ 0.032

Table 1: **Theory-aligned diagnostics on OOD trajectories.** We report empirical approximations for the quantities appearing in the barrier-margin analysis. Bellman satisfaction is the percentage of transitions with  $\Delta_{\text{bell},t} \leq 10^{-6}$ .  $\widehat{Q}_C^+$  denotes the pessimistic critic used by the deployed Q-barrier. Residual magnitudes are reported in critic-scaled cost units. SafetyHalfCheetah has the largest prediction error, which is consistent with its more conservative reward-cost behavior under Q-Barrier shielding.

Environment	Bellman sat. mean $\uparrow$	Bellman sat. $\widehat{Q}_C^+ \uparrow$	$\Delta_{\text{bell}}^{\text{mean}} \downarrow$	$\Delta_{\text{bell}}^+ \downarrow$
SafeDarkRoom	66.7 $\pm$ 1.1	72.2 $\pm$ 1.0	169.0 $\pm$ 8.2	67.19 $\pm$ 3.20
SafeDarkMujoco-Point	93.2 $\pm$ 0.6	89.8 $\pm$ 0.9	0.053 $\pm$ 0.007	0.248 $\pm$ 0.048
SafeDarkMujoco-Car	78.6 $\pm$ 0.5	89.8 $\pm$ 0.4	11.0 $\pm$ 0.51	0.104 $\pm$ 0.004
SafeVelocity-HalfCheetah	72.8 $\pm$ 0.2	70.5 $\pm$ 0.2	0.257 $\pm$ 0.004	0.386 $\pm$ 0.005
SafeVelocity-Ant	88.6 $\pm$ 0.5	89.9 $\pm$ 0.5	1.089 $\pm$ 0.038	0.719 $\pm$ 0.032

Table 2: **Effect of pessimistic critic aggregation on Bellman diagnostics.** We use the same layout in Table 1.

## B Empirical Diagnostics for the Barrier-Margin Analysis

The barrier-margin bound in Theorem 1 depends on learned quantities that are not guaranteed by construction: one-step latent prediction error, local sensitivity of the learned cost critic, and the Bellman upper-bound residual of the critic. We therefore measure these quantities directly on evaluation trajectories using the deployed soft Q-barrier shield with  $N_s = 8$  candidate actions. In the main text,  $\widehat{Q}_C^+$  denotes the pessimistic ensemble critic used by the deployed barrier. In this appendix, we also report diagnostics for the ensemble mean critic  $\widehat{Q}_C^{\text{mean}}$  to isolate the effect of pessimistic aggregation. We omit  $k$  for notational simplicity.

For each selected transition  $(Z_t^w, A_t, C_{t+1}, Z_{t+1}^w)$ , we compute the one-step latent prediction error

$$e_{\text{pred},t} = \|f_z(Z_t^w, A_t) - Z_{t+1}^w\|_2. \quad (18)$$

To evaluate the value perturbation induced by this latent error, we use the same next-step candidate set  $\mathcal{A}_{t+1}^{\text{cand}}$  for both the predicted and realized next latent states:

$$\widehat{V}_{C,t+1}^+(Z) = \min_{A' \in \mathcal{A}_{t+1}^{\text{cand}}} \widehat{Q}_C^+(Z, A'). \quad (19)$$

The directly induced value perturbation is

$$e_{V,t}^+ = \left| \widehat{V}_{C,t+1}^+(f_z(Z_t^w, A_t)) - \widehat{V}_{C,t+1}^+(Z_{t+1}^w) \right|. \quad (20)$$

This is the most direct empirical analogue of the value perturbation term in Lemma 1.

We also report a finite-difference proxy for local critic sensitivity:

$$\widehat{L}_{Q,t}^{\text{local},+} = \max_{A' \in \mathcal{A}_{t+1}^{\text{cand}}} \frac{\left| \widehat{Q}_C^+(f_z(Z_t^w, A_t), A') - \widehat{Q}_C^+(Z_{t+1}^w, A') \right|}{\|f_z(Z_t^w, A_t) - Z_{t+1}^w\|_2 + \epsilon}, \quad \epsilon = 10^{-8}. \quad (21)$$

This quantity should be interpreted only as a local finite-difference diagnostic: it can become large when the latent prediction error in the denominator is very small. For this reason, we use  $e_{V,t}^+$  as the primary diagnostic for the actual value-estimation perturbation entering the theorem.

Finally, we compute the Bellman upper-bound residual:

$$\Delta_{\text{bell},t}^+ = \left[ C_{t+1} + \widehat{V}_{C,t+1}^+(f_z(Z_t^w, A_t)) - \widehat{Q}_C^+(Z_t^w, A_t) \right]_+. \quad (22)$$

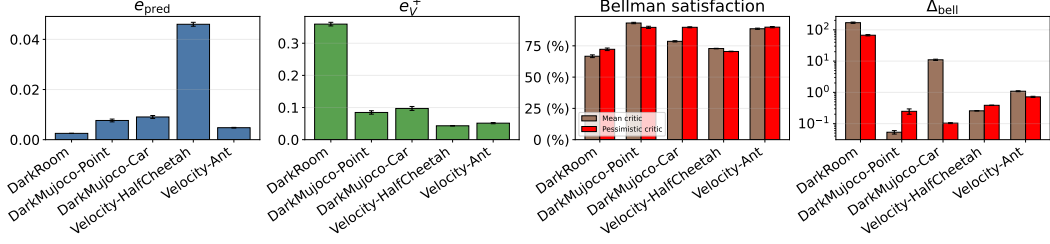


Figure 3: **Theorem-aligned diagnostics on OOD evaluation trajectories.** We report one-step latent prediction error, induced value perturbation, Bellman upper-bound satisfaction, and positive Bellman residual. Error bars show standard error over rollout-level summaries. We compare the ensemble mean critic with the pessimistic critic used by the deployed Q-barrier. Bellman residuals are plotted on a log scale because their magnitudes differ across critic scales and environments.

The cost  $C_{t+1}$  uses the same scaling as critic training. A transition satisfies the learned Bellman upper-bound condition when  $\Delta_{\text{bell},t}^+ \leq 10^{-6}$ . We also compute the same residual for the ensemble mean critic  $\hat{Q}_C^{\text{mean}}$  to isolate the effect of pessimistic aggregation.

All diagnostics are computed after action selection and are not used by the policy or shield during deployment. We first aggregate metrics within each evaluation rollout, using 50 tasks, and then report mean  $\pm$  standard errors across rollouts.

Table 1 shows that the theorem-relevant quantities vary across environments. SafeHalfCheetah has the largest latent prediction error, which is consistent with the more conservative behavior observed in the main experiments. SafeDarkRoom has a small latent prediction error but a large local finite-difference sensitivity and a large Bellman residual in critic-scaled units, indicating that its learned critic changes sharply even under small latent perturbations. This is why we interpret  $\hat{L}_Q^{\text{local},+}$  as a diagnostic rather than as a verified global Lipschitz constant.

Table 2 isolates the effect of pessimistic critic aggregation on the Bellman upper-bound residual. The pessimistic critic improves Bellman satisfaction or reduces residual magnitude in SafeDarkRoom, SafetyCar, and SafetyAnt. The effect is not uniform: in SafetyPoint and SafetyHalfCheetah, pessimistic aggregation slightly lowers Bellman satisfaction and increases the positive residual. This is expected because max aggregation increases predicted cost and therefore acts as a deployment-time safety bias, but it does not by itself enforce Bellman upper-bound consistency on every transition.

These diagnostics should therefore be read as residual measurements for the bound in Theorem 1, not as independent safety certificates. When  $\Delta_{\text{bell}}$  is small and Bellman satisfaction is high, the theorem’s residual term is tighter. When the residual is larger, the barrier-margin statement becomes correspondingly weaker. This distinction is important for SafetyHalfCheetah, where weaker Bellman diagnostics and larger latent prediction error are consistent with the more conservative reward-cost behavior observed in the main experiments.

## C Hard Shield Variant

The main empirical results use the soft shield from Equation (3), which preserves support over the finite candidate set while downweighting actions with negative Q-barrier margin. Here, we report a corresponding hard truncation variant. The hard shield restricts action selection to the barrier-feasible subset of the candidate set whenever that subset is nonempty.

For the realized finite candidate set  $\mathcal{A}_{t,k}^{\text{cand}}$ , define the hard safe set

$$\mathcal{A}_{\text{safe},t}^k(Z_t^{w,k}, B_t^k) \doteq \left\{ A \in \mathcal{A}_{t,k}^{\text{cand}} : b_{Q,t}^k(Z_t^{w,k}, B_t^k, A) \geq 0 \right\} = \left\{ A \in \mathcal{A}_{t,k}^{\text{cand}} : \hat{Q}_C^+(Z_t^{w,k}, A) \leq B_t^k \right\}. \quad (23)$$

As in the soft shield, define the finite-candidate base weight

$$\rho_t(A) = \begin{cases} \pi_\theta(A | Z_t^{p,k}), & \text{if the discrete action space is enumerated,} \\ 1, & \text{if } A \in \mathcal{A}_{t,k}^{\text{cand}} \text{ is sampled from } \pi_\theta(\cdot | Z_t^{p,k}). \end{cases}$$

The hard-shield policy over the finite candidate set is

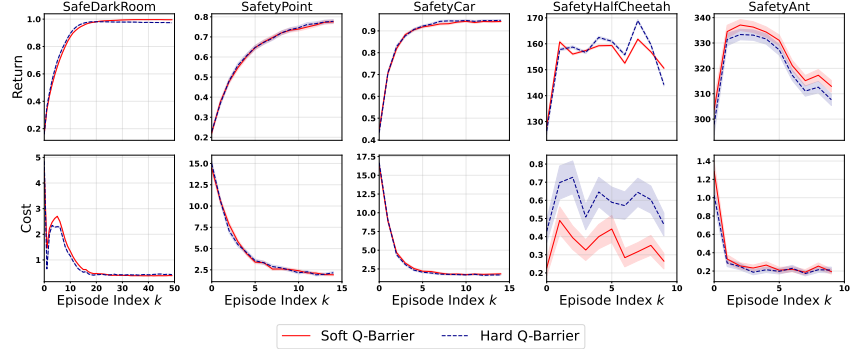
$$\pi_{\text{hard}}(A \mid S_t^k, Z_t^k, B_t^k) = \begin{cases} \frac{\rho_t(A) \mathbb{I}[A \in \mathcal{A}_{\text{safe},t}^k(Z_t^{w,k}, B_t^k)]}{\sum_{A' \in \mathcal{A}_{t,k}^{\text{cand}}} \rho_t(A') \mathbb{I}[A' \in \mathcal{A}_{\text{safe},t}^k(Z_t^{w,k}, B_t^k)]}, & \text{if the denominator} > 0, \\ \frac{\mathbb{I}[A \in \mathcal{A}_{\text{min},t}^k]}{|\mathcal{A}_{\text{min},t}^k|}, & \text{otherwise,} \end{cases} \quad (24)$$

where

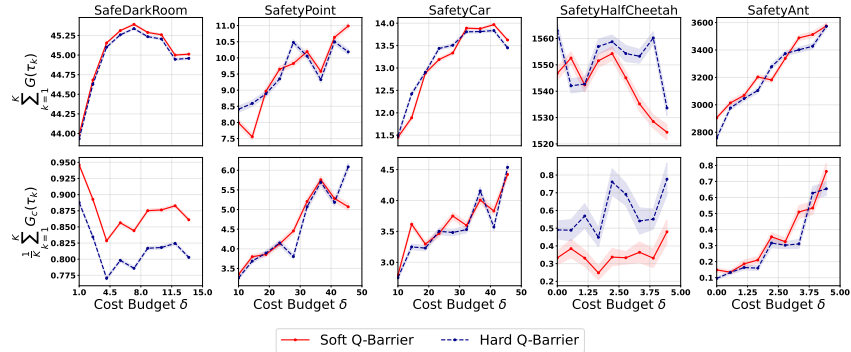
$$\mathcal{A}_{\text{min},t}^k \doteq \arg \min_{A' \in \mathcal{A}_{t,k}^{\text{cand}}} \hat{Q}_C^+(Z_t^{w,k}, A'). \quad (25)$$

If the safe candidate set is nonempty, the hard shield renormalizes the finite-candidate base weights over barrier-feasible candidates only. If the safe set is empty, it falls back to the candidate with the smallest pessimistic predicted cost, with uniform tie-breaking if multiple candidates attain the minimum.

In discrete-action settings,  $\rho_t(A)$  is the base-policy probability mass, so Equation (24) is a standard truncation and renormalization of the backbone policy. In continuous-action settings, the candidate actions are already sampled from the base policy, so  $\rho_t(A) = 1$  and the hard shield is a finite-sample rejection/resampling rule over the sampled candidates. It should therefore be interpreted as a hard filter on the sampled candidate set, not as a truncation of the full continuous policy density.



(a) In-context adaptation dynamics



(b) Reward-cost tradeoffs under budget variation

**Figure 4: Soft versus hard Q-barrier shielding.** We compare the soft shield used in the main experiments with a hard truncation variant that selects only from barrier-feasible candidates when possible. The two variants have similar reward–safety profiles in most environments. Hard shielding gives marginal cost reductions in several environments, such as SafeDarkRoom, but these gains can come with small return loss and are not uniform. In SafetyHalfCheetah, hard shielding achieves the highest return but also increases cost, consistent with the larger latent prediction error reported in Table 1. This suggests that hard truncation is not automatically safer when the learned barrier is affected by model or critic error.

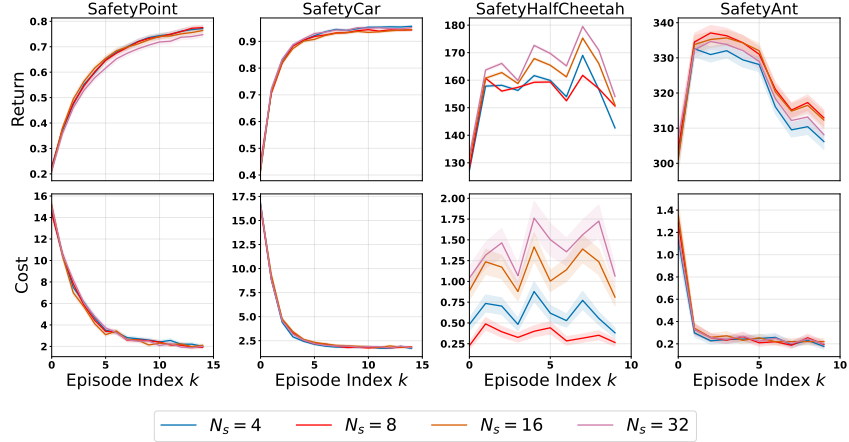
## D Ablation: Hard Q-Barrier vs. Soft Q-Barrier

The main experiments use the soft Q-barrier shield from Equation (3). The soft shield preserves support over the finite candidate set by exponentially downweighting actions with negative barrier margin. In contrast, the hard shield from Equation (24) truncates the candidate distribution to actions that satisfy the learned barrier whenever such actions exist, and otherwise falls back to the candidate with the smallest pessimistic predicted cost. Both variants are deployment-time action-selection rules and use the same pretrained model, base policy, encoder, latent dynamics model, and pessimistic cost critic. We evaluate both shield types on the OOD tasks from the main experiments. The only difference between the two variants is the deployment-time action-selection rule: soft reweighting versus hard truncation. All other components are shared.

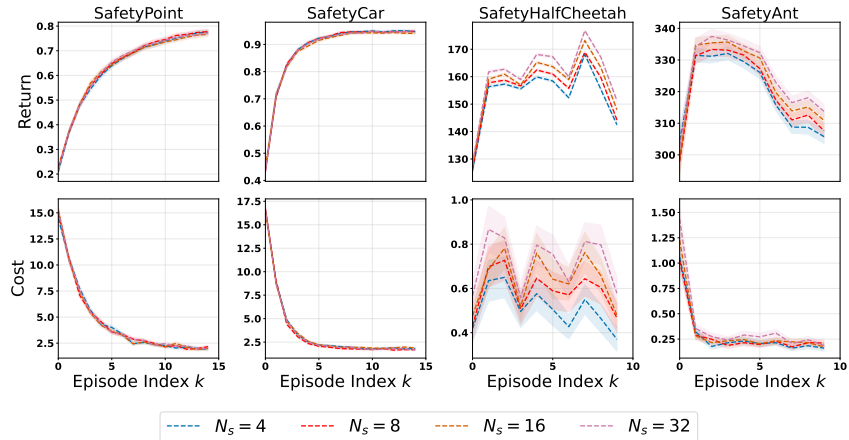
Figure 4 shows that hard and soft shielding perform similarly overall. In SafeDarkRoom, hard shielding slightly reduces cost relative to soft shielding, but with a small return drop, suggesting that the soft shield already assigns most probability to low-risk candidates.

SafetyHalfCheetah is the main exception: hard shielding achieves higher return than soft shielding, but also increases cost. This is consistent with the diagnostics in Table 1, where SafetyHalfCheetah has the largest latent prediction error. With less accurate latent prediction, hard thresholding can be less stable: small barrier errors may flip candidates between safe and unsafe, and fallback or truncation can amplify these mistakes. Soft shielding is smoother because it changes candidate probabilities continuously with the predicted barrier margin.

Overall, this ablation supports using the soft shield in the main experiments. Hard shielding can slightly reduce cost in some cases, but the gains are small and inconsistent. Soft shielding provides a more stable deployment-time tradeoff by biasing selection toward lower predicted cost while avoiding the discontinuities and empty-safe-set fallback behavior of hard filtering.



(a) Soft Q-Barrier



(b) Hard Q-Barrier

Figure 5: **Effect of candidate-set size on OOD adaptation dynamics.** We vary the number of sampled candidate actions  $N_s \in \{4, 8, 16, 32\}$  used by our Q-barrier shield during deployment. **(a)** soft filtering, which reweights candidates by their barrier values, and **(b)** hard filtering, which removes candidates that fail the barrier test. Curves show per-episode return and cost over the in-context OOD evaluation horizon, with shaded regions denoting standard errors across rollouts.

## E Number of Candidate Actions in Continuous Control

The Q-barrier shield evaluates a finite candidate set before selecting an action. In discrete-action environments this set is the full action space, but in continuous-action environments the shield approximates the budget-aware action distribution using  $N_s$  actions sampled from the base policy. This ablation studies how the number of sampled candidates affects the reward-safety tradeoff.

We evaluate  $N_s \in \{4, 8, 16, 32\}$  on the continuous-control environments including SafeDarkMujoco and SafeVelocity domains. For each  $N_s$ , we compare the soft shield used in the main experiments with a hard shield that rejects candidate actions whose learned Q-barrier is negative whenever possible.

Figure 5 studies the effect of the number of sampled candidate actions  $N_s$  under soft and hard Q-barrier shielding. The sensitivity is environment dependent. In SafeDarkMujoco, both return and cost are stable across  $N_s$  for both filtering rules. Hard filtering (Figure 5b) is especially insensitive because it removes candidates that fail the learned barrier test, so larger candidate sets mainly affect which feasible action is selected. Soft filtering (Figure 5a) instead reweights all sampled candidates

according to their barrier values, making the selected action more susceptible to additional high-return but higher-cost samples.

The SafeVelocity environments show a stronger sampling effect. In SafetyHalfCheetah, increasing  $N_s$  improves return during adaptation, but also increases cost. This reward-cost tradeoff is more ordered under hard filtering: larger candidate sets consistently increase return, at the expense of higher cost, in both SafetyHalfCheetah and SafetyAnt. Under soft filtering, the ordering is less consistent because unsafe or near-unsafe candidates are downweighted rather than removed, leaving more dependence on the learned barrier scale. The stronger sensitivity in locomotion is expected, since these tasks have higher-dimensional action spaces and a finite candidate set more directly limits the shield’s ability to find high-return safe actions. Overall, the ablation supports using  $N_s = 8$  as a conservative default in the main experiments. We do not tune  $N_s$  per environment or report the best sampling number.

## F Pseudocode

We provide pseudocode for the training procedure and the deployment-time action-selection rule used by the proposed shielding framework. Algorithm 1 summarizes the training pipeline, including the base actor-critic update together with the auxiliary latent/world-model objectives. Algorithm 2 summarizes the runtime Q-barrier shielding rule used at deployment.

---

### Algorithm 1 Training Procedure

---

**Require:** Batch of history-conditioned trajectories  $\mathcal{B}$

- 1: Initialize shared encoder  $E_\phi$ , policy head  $\pi_\theta$ , reward critic ensemble  $\{\hat{Q}_{R,i}\}_{i=1}^M$ , cost critic ensemble  $\{\hat{Q}_{C,i}\}_{i=1}^M$ , and target copies  $\bar{\pi}_\theta$ ,  $\{\bar{Q}_{R,i}\}_{i=1}^M$ ,  $\{\bar{Q}_{C,i}\}_{i=1}^M$
  - 2: Initialize projection heads  $g_\omega^{\text{world}}$ ,  $g_\psi^{\text{policy}}$
  - 3: Initialize latent dynamics model  $p_z$ , reward head  $\hat{R}$ , and cost head  $\hat{C}$
  - 4: **for** each training update **do**
  - 5:   Sample batch  $\mathcal{B}$  of padded trajectories indexed by  $(k, t)$
  - 6:   Encode transitions:  $Z_t^k \leftarrow E_\phi(H_t^k, S_t^k)$  and  $Z_{t+1}^k \leftarrow E_\phi(H_{t+1}^k, S_{t+1}^k)$
  - 7:   Project to world and policy latents:
 
$$\begin{aligned} Z_t^{w,k} &\leftarrow g_\omega^{\text{world}}(Z_t^k), & Z_{t+1}^{w,k} &\leftarrow g_\omega^{\text{world}}(Z_{t+1}^k) \\ Z_t^{p,k} &\leftarrow g_\psi^{\text{policy}}(Z_t^k), & Z_{t+1}^{p,k} &\leftarrow g_\psi^{\text{policy}}(Z_{t+1}^k) \end{aligned}$$
  - 8:   Compute policy outputs  $\pi_\theta(\cdot | Z_t^{p,k})$
  - 9:   Compute world-model outputs:
 
$$f_z(Z_t^{w,k}, A_t^k), \quad \text{predicted reward } \hat{R}_{t+1}^k, \quad \text{predicted cost } \hat{C}_{t+1}^k$$
  - 10:   Sample target action  $A'_{t+1} \sim \bar{\pi}_\theta(\cdot | Z_{t+1}^{p,k})$
  - 11:   Compute detached Bellman targets:
 
$$\begin{aligned} Y_t^R &\leftarrow R_{t+1}^k + \gamma(1 - D_{t+1}^k) \frac{1}{M} \sum \bar{Q}_{R,j}(Z_{t+1}^k, A'_{t+1}) \\ Y_t^C &\leftarrow C_{t+1}^k + \gamma(1 - D_{t+1}^{\text{ctx}}) \frac{1}{M} \sum \bar{Q}_{C,j}(Z_{t+1}^{w,k}, A'_{t+1}) \end{aligned}$$
  - 12:   Compute critic loss:
 
$$\mathcal{L}_{\text{critic}} \leftarrow \frac{1}{M} \sum_{i=1}^M \left[ \left( \hat{Q}_{R,i}(Z_t^k, A_t^k) - Y_t^R \right)^2 + \left( \hat{Q}_{C,i}(Z_t^{w,k}, A_t^k) - Y_t^C \right)^2 \right]$$
  - 13:   Compute actor loss:
 
$$\mathcal{L}_{\text{actor}} \leftarrow \mathcal{L}_{\text{DPG}} + \alpha_{\text{BC}} \mathcal{L}_{\text{AWBC}} + \lambda_C \mathcal{L}_C^\pi$$
  - 14:   Compute world-model loss  $\mathcal{L}_{\text{wm}}$
  - 15:   Compute distillation loss  $\mathcal{L}_{\text{distill}}^{\text{sg}}$
  - 16:   Compute conjugacy loss  $\mathcal{L}_{\text{conj}}^{\text{sg}}$
  - 17:    $\mathcal{L}_{\text{total}} \leftarrow \mathcal{L}_{\text{actor}} + 10.0 \mathcal{L}_{\text{critic}} + 1.0 \mathcal{L}_{\text{wm}} + 0.1 \mathcal{L}_{\text{distill}}^{\text{sg}} + 0.1 \mathcal{L}_{\text{conj}}^{\text{sg}}$
  - 18:   Update trainable parameters using  $\nabla \mathcal{L}_{\text{total}}$
  - 19:   Update target networks by Polyak averaging
  - 20: **end for**
- 

Here  $\mathcal{L}_{\text{DPG}}$  is the online policy-improvement loss,  $\mathcal{L}_{\text{AWBC}}$  is the advantage-filtered behavioral cloning loss, and  $\mathcal{L}_C^\pi$  is the Lagrangian cost penalty computed from the pessimistic cost critic. We

use  $M = 4$  critics, one target action sample, and  $\alpha_{BC} = 0.1$ . Bellman targets are computed with Polyak-averaged target networks and detached from the critic update.

**Remark.** SCARED uses the same base policy training pipeline as Q-Barrier, including the actor/critic updates, target networks, target-conditioning protocol, and training schedule. The difference is that Q-Barrier augments this backbone with shield-specific modules and losses: the world/policy projections, latent dynamics model, reward/cost prediction heads, structural alignment losses, and the runtime Q-barrier action-selection rule.

---

**Algorithm 2** Q-Barrier Shielding for Finite Candidate Action Selection

---

**Require:** State  $S_t^k$ , context  $H_t^k$ , budget  $\delta$ , frozen policy  $\pi_{\theta_*}$ , ensemble critics  $\{\hat{Q}_{C,i}\}_{i=1}^N$ , shield type  $q \in \{\text{soft}, \text{hard}\}$

- 1: Encode shared latent:  $Z_t^k \leftarrow E_\phi(H_t^k, S_t^k)$
- 2: Project latents:  $Z_t^{w,k} \leftarrow g_\omega^{\text{world}}(Z_t^k)$ ,  $Z_t^{p,k} \leftarrow g_\psi^{\text{policy}}(Z_t^k)$
- 3: Compute remaining budget:  $B_t^k \leftarrow \delta - \sum_{\tau=1}^t C_\tau^k$
- 4: **if** action space is discrete **then**
- 5:    $\mathcal{A}_{t,k}^{\text{cand}} \leftarrow \mathcal{A}$
- 6:    $\rho_t(A) \leftarrow \pi_{\theta_*}(A \mid Z_t^{p,k})$  for each  $A \in \mathcal{A}_{t,k}^{\text{cand}}$
- 7: **else**
- 8:   Sample  $\mathcal{A}_{t,k}^{\text{cand}} = \{A^{(j)}\}_{j=1}^{N_s}$  from  $\pi_{\theta_*}(\cdot \mid Z_t^{p,k})$
- 9:    $\rho_t(A) \leftarrow 1$  for each  $A \in \mathcal{A}_{t,k}^{\text{cand}}$
- 10: **end if**
- 11: **for** each  $A \in \mathcal{A}_{t,k}^{\text{cand}}$  **do**
- 12:    $\hat{Q}_C^+(Z_t^{w,k}, A) \leftarrow \max_i \hat{Q}_{C,i}(Z_t^{w,k}, A)$
- 13:    $b_{Q,t}^k(Z_t^{w,k}, B_t^k, A) \leftarrow B_t^k - \hat{Q}_C^+(Z_t^{w,k}, A)$
- 14: **end for**
- 15: **if**  $q = \text{soft}$  **then**
- 16:   **for** each  $A \in \mathcal{A}_{t,k}^{\text{cand}}$  **do**
- 17:      $w_t(A) \leftarrow \rho_t(A) \exp\left(-[-b_{Q,t}^k(Z_t^{w,k}, B_t^k, A)]_+\right)$
- 18:   **end for**
- 19:   Normalize:  $\pi_{\text{soft}}(A) \leftarrow w_t(A) / \sum_{A' \in \mathcal{A}_{t,k}^{\text{cand}}} w_t(A')$
- 20:   **return**  $A_t^k \sim \pi_{\text{soft}}$
- 21: **else**
- 22:    $\mathcal{A}_{\text{safe},t}^k \leftarrow \{A \in \mathcal{A}_{t,k}^{\text{cand}} : b_{Q,t}^k(Z_t^{w,k}, B_t^k, A) \geq 0\}$
- 23:   **if**  $\mathcal{A}_{\text{safe},t}^k \neq \emptyset$  **then**
- 24:     **for** each  $A \in \mathcal{A}_{t,k}^{\text{cand}}$  **do**
- 25:       $w_t(A) \leftarrow \rho_t(A) \mathbb{I}[A \in \mathcal{A}_{\text{safe},t}^k]$
- 26:     **end for**
- 27:     Normalize:  $\pi_{\text{hard}}(A) \leftarrow w_t(A) / \sum_{A' \in \mathcal{A}_{t,k}^{\text{cand}}} w_t(A')$
- 28:     **return**  $A_t^k \sim \pi_{\text{hard}}$
- 29:   **else**
- 30:      $A_{\text{min},t}^k \leftarrow \arg \min_{A \in \mathcal{A}_{t,k}^{\text{cand}}} \hat{Q}_C^+(Z_t^{w,k}, A)$
- 31:     **return**  $A_t^k \sim \text{Uniform}(\mathcal{A}_{\text{min},t}^k)$  ▷ lowest predicted-cost fallback
- 32:   **end if**
- 33: **end if**

---

**Notes on presentation.** Algorithm 1 expands the base history-conditioned actor-critic forward path, making the interaction between policy optimization and auxiliary shielding objectives explicit. Algorithm 2 is the deployment-time rule used by the proposed method: the shield encodes the current state and context into shared and projected latents, computes the remaining budget, evaluates candidate actions with a pessimistic ensemble cost critic, and biases action selection toward actions with nonnegative barrier margin.

## G Environment Details

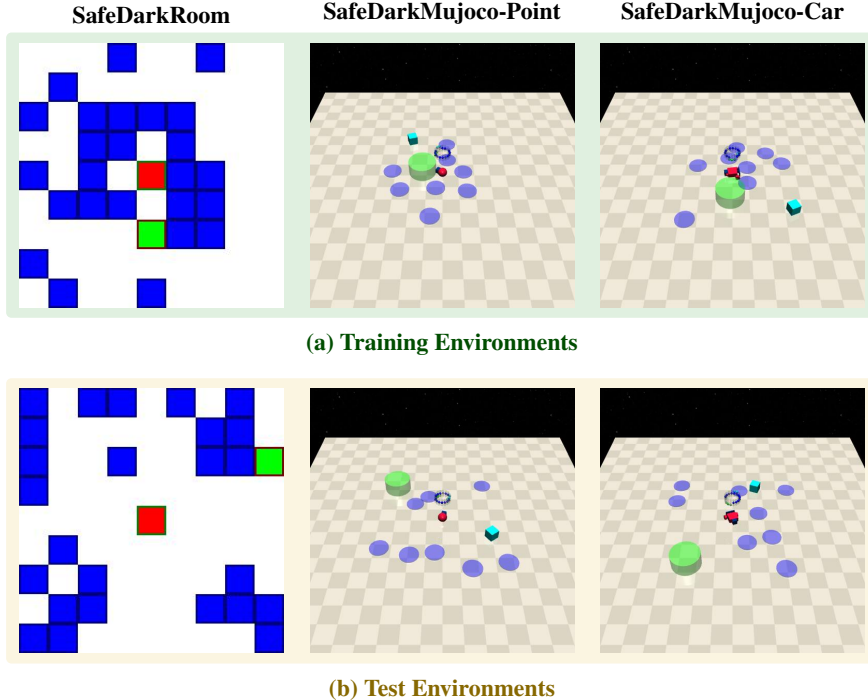


Figure 6: Visualization of the environment layouts, directly adapted from Moeini et al. [40]. The agent (red) must navigate to the target location (green) while avoiding obstacles (blue shades). To evaluate out-of-distribution generalization, training configurations sample goals and obstacles using a center-oriented distribution ( $\alpha=0.5$ ), whereas evaluation configurations strictly employ edge-oriented placements.

**Out-of-Distribution Environment Generation.** For SafeDarkRoom and SafeDarkMujoco, we adopt the distance-based spawning protocol used in the safe ICRL benchmark of Moeini et al. [40]. This benchmark creates a controlled distributional shift by sampling training and evaluation environments from spatial distributions with opposite concentration patterns.

During training, obstacle and goal locations are sampled from a center-concentrated distribution,

$$p_{\text{train}}(x) \propto \exp(-\alpha d(x, c)),$$

where  $d(x, c)$  denotes Euclidean distance from the map center  $c$ . Evaluation environments invert this distribution,

$$p_{\text{test}}(x) \propto \exp(\alpha d(x, c)),$$

forcing the agent to extrapolate into regions that are rarely observed during training. As discussed by Moeini et al. [40], increasing  $\alpha$  sharpens the separation between training and test distributions and makes the resulting shift increasingly severe. We refer readers to that work for the full benchmark construction and derivations. For convenience, Figure 6 reproduces representative training and evaluation layouts.

**Measuring OOD Generalization.** Goal-discovery environments such as DarkRoom are widely used in prior ICRL work [33, 71, 54]. In those settings, test-time generalization is typically evaluated by holding out goal locations during training. However, such held-out tasks may still be solvable by interpolation across nearby training tasks [27].

The structural OOD setup used here is stricter. Rather than withholding individual goals, we change the spatial distribution from which both goals and obstacles are sampled. During training, the agent starts near the map center and encounters center-oriented tasks more often. During evaluation, both goals and obstacles are drawn from edge-oriented distributions. This shift applies to both

SafeDarkRoom and SafeDarkMujoco and is designed to test extrapolative generalization to regions that are systematically underrepresented during training.

**Safe ICRL Benchmarks.** SafeDarkRoom is a partially observed grid-world adaptation of DarkRoom [33]. The agent observes only its own position and cannot directly observe either the goal or the obstacles. Rewards are sparse, and costs arise from stepping on hazards distributed throughout the map. The agent must therefore infer both where to go and where not to go from the reward and cost signals accumulated in context.

SafeDarkMujoco is the continuous-control counterpart built on MuJoCo [56]. The robot observes internal physical states such as position, velocity, acceleration, and rotation angle, but does not receive direct sensing of the goal or obstacles. As in SafeDarkRoom, successful adaptation requires using sparse reward and cost observations from previous interaction to infer the hidden task structure.

SafeVelocity follows the Safety Gym style of safe locomotion tasks [25], but evaluation is performed on held-out target velocities from the same task family. We treat this benchmark as unseen ID generalization rather than structural OOD generalization because the deployment tasks are new parameter settings within the same family, not tasks sampled from a qualitatively shifted spatial distribution.

## H Training Details

**SCARED.** We use the original implementation of Moeini et al. [40]. During SCARED pretraining, we resample a new environment from the training distribution every  $K$  episodes. For each sampled environment, we also sample a CTG target. The CTG range is  $[1, 15]$  for SafeDarkRoom and  $[10, 50]$  for SafeDarkMujoco.

SCARED follows the AMAGO-style history-conditioned architecture of Grigsby et al. [17]. An MLP time-step encoder maps each tuple  $(S_t, A_t, R_t, C_t)$  to an embedding, and a transformer-based trajectory encoder processes the resulting sequence. The prediction head outputs either an action distribution in discrete-action environments or a value prediction in continuous-action environments. Table 3 lists the remaining hyperparameters.

**Q-Barrier.** Shield-supporting modules, including the encoder  $E_\phi$ , projection heads  $g_\omega^{\text{world}}$  and  $g_\psi^{\text{policy}}$ , latent dynamics model  $p_z$ , and ensemble cost critic  $\{\hat{Q}_{C,i}\}_{i=1}^M$ , train jointly with SCARED during pretraining, without additional epochs. In discrete-action environments, the shield evaluates the full action space during training to learn the cost critic and barrier signal. In continuous-control environments, candidate sampling is deferred to deployment: the latent dynamics, cost critic, and projection heads are trained without candidate sampling, which avoids repeated per-update candidate generation. At test time, the frozen shield samples  $N_s$  actions from the base policy and applies the reweighting rule in Algorithm 2. The loss weights in Equation (4) are fixed across all environments:  $\lambda_{\text{critic}} = 10.0$ ,  $\lambda_{\text{wm}} = 1.0$ ,  $\lambda_{\text{dist}} = 0.1$ ,  $\lambda_{\text{conj}} = 0.1$ . Every other parameters exactly follow Table 3.

**SafeMeta and MAML with penalty.** We use the original implementations of Xu and Zhu [64] with three hidden layers of sizes  $(64, 512, 64)$  for the policy, value, and cost networks, for a total of 205,510 parameters. We train for 15k meta-training iterations, sampling 20 tasks from the training distribution at each iteration. During meta-testing, both algorithms perform  $K$  gradient updates to adapt to new tasks with unseen cost-to-go values. Although some meta-RL methods use frame stacking or recurrent architectures, their hidden states reset between episodes; they therefore remain episodic and do not carry information across episode boundaries in the way ICRL methods do.

**Safe Algorithm Distillation.** We use the original implementation of Moeini et al. [40]. For Safe AD, we collect a dataset  $\mathcal{D} = \{\Xi_i\}$  of learning histories, where each trajectory  $\Xi_i \doteq (\tau_1, \tau_2, \dots, \tau_K)$  is a sequence of episodes generated by running safe RL algorithms on CMDPs. Each episode  $\tau_k$  contains states, actions, rewards, and costs.

We train the Safe AD policy autoregressively to distill the behavior present in these logged learning histories, following Laskin et al. [33]. Each training example contains a trajectory segment together with RTG and CTG conditioning. The policy takes as input  $(S_t^k, H_t^k, G_t(\tau_k), G_{c,t}(\tau_k))$  and predicts the action at time  $t$  in episode  $k$ .

Parameter	SafeDarkRoom	SafeDarkMujoco & SafeVelocity
Episode time limit $t_{\max}$	30	75
Replay buffer capacity	100,000	100,000
Embedding dim	64	64
Hidden dim	64	64
Num layers	4	4
Num heads	8	8
Seq len	1500	1500
Attention dropout	0	0
Residual dropout	0	0
Embedding dropout	5	5
Learning rate	$3 \times 10^{-4}$	$3 \times 10^{-4}$
Betas	(0.9, 0.99)	(0.9, 0.99)
Clip grad	1.0	1.0
Batch size	32	32
Optimizer	Adam	Adam

Table 3: Hyperparameters for SCARED.

Parameter	SafeDarkRoom	SafeDarkMujoco & SafeVelocity
Episode time limit $t_{\max}$	30	75
Hidden layers	(64, 512, 64)	(64, 512, 64)
Min/max batch size	500/1500	1500/1500
Policy learning rate	$10^{-3}$	$10^{-3}$
Value/cost learning rate	$3 \times 10^{-2}/10^{-1}$	$3 \times 10^{-2}/10^{-1}$
Discount factor $\gamma$	0.99	0.99
GAE parameter $\tau$	0.95	0.95
Max KL divergence	$10^{-3}$	$10^{-3}$
Lagrangian weight $\lambda$	1.0	1.0
Num meta-training iterations	15k	15k
Policy optimizer	Adam	Adam
Value/cost optimizer	L-BFGS	L-BFGS

Table 4: Hyperparameters for SafeMeta and MAML with penalty.

**Discrete action spaces.** For environments with discrete actions, the model outputs categorical logits and is trained with cross-entropy:

$$\mathcal{L}_{\text{disc}}(\theta) = \mathbb{E}_{\Xi_i \sim \mathcal{D}} \left[ -\log \pi_{\theta}(A_t^k | S_t^k, H_t^k, G_t(\tau_k), G_{c,t}(\tau_k)) \right]. \quad (26)$$

**Continuous action spaces.** For environments with continuous actions, the model predicts an action mean and is trained with an  $\ell_2$  regression loss:

$$\mathcal{L}_{\text{cont}}(\theta) = \mathbb{E}_{\Xi_i \sim \mathcal{D}} \left[ \left\| A_t^k - \mu_{\theta}(S_t^k, H_t^k, G_t(\tau_k), G_{c,t}(\tau_k)) \right\|_2^2 \right]. \quad (27)$$

These objectives let the transformer absorb constraint-aware goal-seeking behavior into its forward pass.

**Dataset collection.** We follow the same training protocol from [40]. We collect Safe AD data by running PPO-Lagrangian [48, 46] on the training environments. For SafeDarkRoom, we vary the cost limit across  $\{0, 2.5, 5.0\}$  and collect 50,000 steps of learning history for each setting. For SafeDarkMujoco and SafeVelocity, we use larger datasets of 2–5 million environment steps to capture a broader range of safety-relevant behavior in continuous control. In these continuous-control environments, we keep the cost limit fixed at 0 during data collection so that the logged histories cover the full trajectory from high-cost exploration to near-feasible behavior later in training. This larger and more behaviorally diverse dataset is necessary because conditioning jointly on RTG and CTG induces a large space of reward-cost tradeoffs that the model must represent.

**Compute resources.** All experiments were run on NVIDIA A100 (80GB) or H100 (80GB) GPUs. SCARED pretraining uses 3K epochs for SafeDarkRoom, and SafeDarkMujoco, and 2K for SafeVel-

<b>Parameter</b>	<b>SafeDarkRoom</b>	<b>SafeDarkMujoco &amp; SafeVelocity</b>
Embedding dim	64	512
Hidden dim	512	256
Num layers	8	8
Num heads	8	8
Seq len	100	200
Attention dropout	0.5	0.5
Residual dropout	0.1	0.1
Embedding dropout	0.3	0.3
Learning rate	$3 \times 10^{-4}$	$3 \times 10^{-4}$
Betas	(0.9, 0.99)	(0.9, 0.99)
Clip grad	1.0	1.0
Batch size	512	128
Optimizer	Adam	Adam

Table 5: Hyperparameters for Safe Algorithm Distillation.

ocity, with the shield-supporting modules (encoder, projection heads, latent dynamics, ensemble cost critic) trained jointly during the same pretraining phase. Safe AD data collection via PPO-Lagrangian requires 2–5 million environment steps per environment. Safe meta-RL baselines (SafeMeta, MAML with penalty) train for up to 15K meta-training iterations.